# POLITECNICO DI TORINO

Master degree course in Mechatronic Engineering

Master Degree Thesis



# Cartography of edaphic variability from RPAS (drones)

**Supervisor**                                          **Candidate**

prof. Marcello CHIABERGE                    Simone GIROTTI


**Internship Supervisors**

Julián Antonio PUCHETA

Néstor DI LEO

*"Anything you can do, or dream you do, begin it: boldness has genius, power, and magic in it."*

**Johann Wolfgang von Goethe**

# Abstract

This project, thanks to the use of RPAS (Remotely Piloted Aircraft System), focus to the investigation about the conditions of variability that can be detected at the soil level, with the aim of identifying areas of homogeneous management of crops so that act automatic or semi-automatic agricultural machines.

Advances in technologies such as Global Positioning Systems (GPS, Galileo), Geographic Information Systems (GIS) and Remote Sensing (RS) instruments make it possible to estimate and characterize this spatial and temporal variability present in the production lot and its management through the use of appropriate strategies.

This scenario brings to a Precision Agriculture strategies with several advantages such as the optimization of the efficiency in the use of supply maximizing the economic benefit, minimization of the risks of contamination of the environment by the application of overdose of items, etc.

The project is developed in an Experimental Field with harvest crops, using aerial robots equipped with multispectral cameras and GNSS (Global Navigation Satellite System) systems.

Aerial and ortho-mosaic photographs is going to be obtained. Vegetation indexes (VI) derived from the reflectivity ortho-mosaics is used; in particular, the NDVI (Normalized Difference Vegetation Index) and the GNDVI (Green Normalized Difference Vegetation Index) are analyzed.

The reliability of the VI data obtained from the elaboration of the multispectral camera's photos are verified in loco thanks to the implementation of various techniques: penetrometry, structural stability and infiltrometry.

From this information, construct the cartography of the edaphic variability and study the most useful way to manage these cartographies to choose the best path that the machinery should follow to do its work optimizing the available resources. This is solved by creating algorithms, capable of implementing operations that allow the autonomous driving in the "actuators" machines.

Finally, the performed simulations will be shown, substantiating the choices done and some design limitations while supporting further developments.

# Table of Contents

# List of Figures and Tables

# Acronyms

BCD        Boustrophedon Cell Decomposition

CPP        Coverage Path Planning

DSM        Digital Surface Model

ED        Edaphic Variable

EF        Experimental Field

FCA        Agricultural Science Faculty

FMI        Farm Management System

GIS        Geographic Information Systems

GNDVI        Green Normalized Difference Vegetation Index

GPS        Global Positioning Systems

ICT        Information and Communication Technology

MZ        Management Zones

NDVI        Normalized Difference Vegetation Index

PA        Precision Agriculture

PP        Path Planning

RPAS        Remotely Piloted Aircraft System

RS        Remote Sensing

SPT        Standard Penetration Test

SSM        Site-Specific Management

TSP        Traveling Salesman Problem

UAV        Unnamed Aerial Vehicles

UNR        Rosario National University

USDA        United State Department of Agriculture

VI        Vegetation Index

# 1. Introduction

## 1.1. Generality

The main idea of the project is to investigate about the conditions of variability that can be detected at the sub-area level, from the use of RPAS (Remotely Piloted Aircraft System), with the aim of identifying areas of homogeneous management of crops so that act automatic or semi-automatic agricultural machines.

It is widely recognized among farmers and technicians that the characteristics of the soil, the presence and type of pests, the yields of a crop and other parameters of agronomic interest are not homogeneous within the same batch (Maroni et al., 2000). Agricultural production systems are inherently variable due to spatial variability in soil properties, topography, climatic conditions, etc.

In order to achieve the sustainability of production systems, variability must necessarily be considered in spatial and temporal dimensions because the variables that influence performance have different behaviours in both dimensions (Verhaegen & Bouma, 1997; & Nowak, 1999).

Advances in technologies such as Global Positioning Systems (GPS, Galileo), Geographic Information Systems (GIS) and Remote Sensing (RS) instruments make it possible to estimate and characterize this spatial and temporal variability present in the production lot and its management through the use of appropriate strategies (Pierce et al., 1997, Basso et al., 2001).

## 1.2. Goals

GENERAL:

- Determine or design a detection system for the edaphic variability at the intra-lot level, using aerial remote sensors.

SPECIFICS:

- Apply the captured images from aerial robots (drones) in the establishment of correlations between the biophysical parameters and the eco-physiological conditions of the crops.

- Apply the edaphic variables that determine differences in the eco-physiological behaviour of the crops surveyed.

- Map the edaphic variables that determine differences in the eco-physiological behaviour of the crops.

- Establish Management Zones (MZ) and implement algorithms to establish the best path within them.

## 1.3. Conceptual Frameworks

The doubling of the world demand for food for the next 50 years poses enormous challenges for the social and environmental sustainability of their production, in relation to the rest of the services provided by terrestrial and aquatic ecosystems to the society. Thus, new incentives and policies to guarantee the sustainability of agriculture will be crucial if we want to meet the demands of improving yields without compromising the integrity of the environment or public health. (Tilman et al., 2002)

On the other hand, the so-called information and communication technology (ICT) has become increasingly vital in the development of modern agriculture, having noted that the increase in yields depends not only on the quality of the soil and the climate, but increasingly from the collection and use of accurate information. In the context of the management of a production system, ICT created systems aimed at obtaining and digitizing statistics, whose analysis reduces risk, improves the efficiency of making decisions and simplifies the implementation of best practices. That is why the use of these computer systems to capture and analyse information has spread, which among other things has allowed the development of models for the optimal application of pesticides,

fertilizers and other supplies, combining physical, biological and chemical safe and environmentally compatible strategies. The most advanced application of these technologies is found in the so-called Precision Agriculture (PA) (Auernhammer, 2001, Cox, 2002, Moguillansky, 2005, Sørensen & Bochtis, 2009), also closely linked to the concept of Agromatic, which means the application from the principles and techniques of computing to the theories and laws of the control and management of agricultural systems, be they a lot, a company or a whole region (Grenón, 1994).

The PA is the culminating point of a wider and comprehensive concept of Site-Specific Management (SSM) of agronomic practices at the productive plot scale. Therefore, the SSM provides the "spatial dimension" to traditional crop management and is defined as "electronic control and monitoring applied to data collection, information processing and decision support, for time and space location of supply in crop production" (Lowenberg-DeBoer & Swinton, 1997).

According to Pierce & Novak (1999), the PA is "the application of technologies and principles to manage the spatial and temporal variability associated with aspects of agricultural production, with the purpose of improving crop yields and environmental quality." The first critical point of the PA is to determine that spatial and/or temporal variability in the edaphic properties or in the crop, quantify its magnitude and evaluate the possibility of managing them through differentiated practices per specific site, which result in benefits compared to traditional uniform management (Melchiori, 2007). Indeed, in the mid-twentieth century, was extended the use of so-called "technological packages" in the national agricultural sector, including aspects such as mechanization, plant breeding and biotechnology, integrated pest management and fertilization. These more or less organized sets of technical recommendations involved their application in the form of uniform treatments of the management units or productive plots (Cox et al., 1999), but the producers quickly noticed that the response of the crops to the applied technological package it was not uniform within each productive plot.

In this sense, the PA allows the implementation of site-specific management strategies to address the spatial-temporal variability of agricultural production (Pierce & Nowak, 1999), which would favour increases in cost-effectiveness by adjusting, for example, the fertilizer doses according to the type of soil and other environmental conditions, but these potential benefits are highly dependent on the precision in the estimation of that variability. According to Hatfield (2000), the variability of yields inside a lot is due to the interaction between different sources of variability, which generate effects that are not always in accordance with the limits established for a lot. One of the purposes of precision agriculture is to identify different environments with similar qualities, determined mainly by topography and edaphic characteristics, which are called management zones (MZ).

The concept of MZ defines sub-regions in a productive plot that express a relatively homogeneous combination of performance factors for which a unique combination of specific inputs is appropriate (Deorge, 1999, Brase, 2006). Thus, each MZ would have to manifests homogeneous characteristics in similar performances, which would allow to optimize the efficiency in the use of supply and to maximize the economic benefit; minimizing risks of contamination of the environment by the application of overdose of items (Dampney & Moore, 1998; Luchiari et al., 2000; Zubillaga et al., 2006).

In summary, precision agriculture can be considered as a three-phase cycle. The first one involves the georeferenced data collection (through Global Positioning Systems - GPS), and the characterization of various parameters that correspond to each MZ. In an initial stage of adoption of this technology, the collection of information will help distinguish and determine the different MZ within the productive plots. Some examples of data normally collected in PA are performance mappings, soil sampling, surveys of farming and health crops conditions on-site or by remote sensing, recording of climate data, etc. (Brase, 2006; Chen et al., 2008).

The second phase involves the interpretation of the data or its analysis. It includes the processes of organization, manipulation, consultation and synthesis of the same. The raw data can involve a large number of numbers and therefore present difficulties for its interpretation. The use of specific tools can help to synthesize and identify the relationships between the variables that the user can use to make a decision (Brase, 2006). This step is very difficult to automate, which means that users have to make decisions with respect to certain agronomic criteria that are capable of understanding the complexity of systemic interrelations involving the soil-plant-atmosphere system, its means, in the environment at the crop level.

The third phase is the one of the implementations. It is about the parameter's adjustment referring to farming operations and the execution of the necessary actions through devices that allow a continuous variation of the application of supplies (Gil, 2004; Brase, 2006). This phase can also be called as "actuation", since it is at this point that the decision made in the previous phase is applied and implemented. This phase will act as feedback providing information for the new phase of data collection of the next PA cycle.

As already mentioned, remote sensors are a complementary and easily accessible alternative for estimating environmental variability and/or productivity, by using reflectivity measures from which result vegetation indexes (VI) that estimate the growth and crop productivity (Zhang et al., 1998; León, 2003). The use of drones to carry remote sensors has gained great popularity in recent years, in applications linked to PA.

In intensive agriculture production systems, machinery investment is one of the largest investments on most farms after real estate, while annual machinery cost is a significant part of a farm's total annual costs (Kay, Edwards, and Duffy, 2008). Nevertheless, mechanization and automatization in agriculture dramatically changed the production costs, efficiency and quality levels and resource optimization.

As the farming machines are traditionally driven by a human, the driver chose the adequate strategy based on type of task and, especially, on his past experiences. However, there could be conditions, e.g. complex field shape and obstacles in it, where human planning can lead to low efficiency. In such cases, implementing path planning algorithms for automated field machinery, can bring excellent benefits (A. Bakhtiari, H. Navid, J. Mehri, D. Bochtis, 2011).

## 1.4. Methodology

The project will be developed in the Experimental Field of the Agricultural Science Faculty of the Rosario National University (FCA-UNR), located in the town of Zavalla, Santa Fe (33° 02' 06.2" S, 60° 54' 11.3" W). Through the use of aerial robots equipped with multispectral cameras and GNSS (Global Navigation Satellite System) systems, flight missions will be structured and planned on lots occupied with harvest crops.

Once the aerial and ortho-mosaic photographs have been obtained, it will be possible to analyse them and define all the elements that arise to the attention and that are considered useful to be highlighted. For this, vegetation indexes (VI) derived from the reflectivity ortho-mosaics will be used; among them, the NDVI (Normalized Difference Vegetation Index) is an index suitable for the study of crops and vegetation in general (Rouse et al., 1974) and one of the VI most used for the estimation of crop yield (Moges et al., 2004). It is also mentioned that a variant of the previous one, the GNDVI (Green Normalized Difference Vegetation Index) has presented correlations with yield in summer grasses (Shanahan et al., 2001).

Both vegetation indexes will be used, and the UAVs (Unnamed Aerial Vehicles) will be adopted as a source, which allows better precision in all parameters due to their greater spatial and temporal resolution (Roberts et al., 1997). The aim is to verify the differences in productivity revealed by the monitoring of performance and those calculated from the VI obtained from remote sensing (Kemerer, 2003), to complete the First Phase of the PA cycle.

The VI data obtained from the elaboration of the multispectral camera's photos must be verified in loco thanks to the implementation of various techniques. Those techniques make use of various tools such as the penetrometer to perform a test that determines the geotechnical characteristics of the soil, as well as the study of the structural stability; or the so-called infiltrometry to evaluate the capacity of the soil to drain the water and so the nutrients.

From this information, construct the cartography of the edaphic variability and study the most useful way to manage these cartographies to choose the best path that the machinery should follow to do its work optimizing the available resources. This will be solved by creating algorithms, capable of implementing the aforementioned operations, in the "actuators" machines, that are intervening in the Third Phase of the PA.

## 1.5. Scope

The present project aims to study the use of Remote Sensors on board of aerial robots (drones) with respect to the First Phase of the Precision Agriculture cycle, as detailed in the theoretical framework.

The starting supplies are the aircraft, with which to get the aerial photos and everything linked to its operation including software (Chapter 2 and Chapter 3) and the tools to obtains data on vegetation variables (Chapter 4).

These data set, photo shoots and soil data, are obtained in loco, an experimental field in Zavalla, Santa Fe. Two expeditions, on the same area, were carried out, one on August 15th and one on October 5th.

The final goal of the project specifically points to the establishment of correlations between the biophysical parameters that can be surveyed by multispectral cameras, and the eco-physiological conditions of the crops. By means of these, to be able to infer conditions of spatial variability in the edaphic characteristics that later make possible the Second and Third Phase of the PA, that is to say the identification of the causes and the determination of the real

management measures to address that spatial variability with criteria of economic and environmental efficiency and sustainability.

Following the cannons of efficiency and sustainability a different Coverage Path Algorithms are going to be analysed in order to offer a further possibility to develop and implement them on an agricultural machinery and make it independent from humans' manual control; a sort of a Smart Agriculture.

An important precondition about this project is that it was not possible to work with an agricultural machinery and its relative devices, for a lack of time and adequate tools, so the path planification will not be an algorithm ready to be implemented on a tractor, but the goal is to represent different feasible solutions available nowadays.

## 1.6.   Overview of Contents

This thesis contains five parts:

About RPAS and Camera Sensors (Chapter 2), Photo Shots by RPAS (Chapter 3), Post-flight photo processing (Chapter 4), Path Planning Algorithm (Chapter 5), Conclusions and Future Developments (Chapter 6).

In Chapter 2, the aircraft and camera sensors main features are listed. In particular it explains how it works and which are the exploited functions.

In Chapter 3, the flight mission planning is described and how the flight software communicates with the UAV and how to set the main parameters according to the needs. A short simulation is carried out.

In Chapter 4, the aerial photos are elaborated to provide a suitable data set to works with. Some Vegetation Index are calculated and further exported in order to obtain a file containing all the important details of the experimental field. The reliability of VI data are analysed by determining the geotechnical characteristics of the soil.

In Chapter 5, different approach to solve the path planning problem are analysed. Starting from the study of the field and vehicle turning a bottom-up algorithm is elaborated. The driving is started by following one edge of the field and possible routes are simulated and the best of these is applied. This is continued until the whole field is covered by the operation.

In Chapter 6, final notions and some possible development strategies are listed.

# 2.  About RPAS and Camera Sensors

## 2.1.  Introduction

The drone used for taking the aerial photos is the "eBee SQ" drone manufactured by senseFly from Parrot Group.

It mounts, the "Parrot Sequoia" camera, produced by the same company, an integrated camera kit equipped with four multispectral sensors plus one RGB sensor a sunshine sensor and integrate also a Global Positioning System (GPS).

This kind of drone is a variant of an RPAS (Remotely Piloted Aircraft Systems). In fact, the drone is remotely piloted but not by a human, it is controlled by a computer; it means that the human plans the flight missions and the PC manage the flight processes.

In the next chapters the terms drone, UAV, RPAS, aircraft and eBee SQ are going to be used as synonyms, just to not misunderstand the concepts.

## 2.2.  eBee SQ

The eBee SQ drone captures harvest data through four multispectral cameras and an RGB sensor, providing reliable insights into the real health of your crops. The drone can cover a lot of hectares in a single flight minimizing the time spent in crop analysis.

A short description about drone specification and key features will follow[1].

---

[1] reference: www.senseFly.com

| HARDWARE | |
| --- | --- |
| Wingspan | 110 cm (43.3 in) |
| Weight | 1.1 kg (2.42 lb) |
| Motor | Low-noise, brushless, electric |
| Ground modem | 2.4 GHz USB |
| Radio link range | 3 km nominal (up to 8 km[1]) / 1.86 mi (up to 4.97 mi[1]) |
| Detachable wings | Yes |
| Sensor (supplied)[2] | Parrot Sequoia |
| Accessories (optional) | Radio tracker, backpack, camera protection kit |
| SOFTWARE | |
| Flight planning & control software (supplied) | eMotion Ag |
| Image processing software (optional) | Pix4Dmapper Pro/Ag, MicaSense Atlas |
| OPERATION | |
| Automatic 3D flight planning | Yes |
| Cruise speed | 40-110 km/h (11-30 m/s or 25-68 mph) |
| Wind resistance | Up to 45 km/h (12m/s or 28 mph) |
| Maximum flight time | 55 minutes |
| Automatic landing | Linear landing with ~ 5 m (16.4 ft) accuracy |
| Ground control points (GCPs) | Optional |
| Hand launch (no catapult required) | Yes |
| RESULTS | |
| **Nominal coverage at 120 m (400 ft)[3]** | 200 ha (~500 ac) |
| GSD multispectral | 12 cm/px (4.72 in/px) |
| GSD RGB | 3.1 cm/px (1.22 in/px) |
| **Maximum coverage at 2,000 m (6,500 ft)[4]** | 3,000 ha (~7,400 ac) |
| GSD multispectral | 2 m/px (6.56 ft/px) |
| GSD RGB | 55 cm/px (21.65 in/px) |

*Fig. 1 eBee SQ Technical specifications*

The eBee SQ has a large compatibility with the most Farm Management System (FMI), agriculture machinery and workflow.

## 2.3. Parrot Sequoia



*Fig. 2 Parrot Sequoia camera*

The Parrot Sequoia is one of the smallest, lightest and accurate multispectral drone sensor. It captures images of yields across four highly defined, visible and non-visible spectral bands, plus RGB imagery, in just one flight[2].

KEY FEATURES:

- Four 1.2 MP sensors (near-infrared, red-edge, red and green) + one 16 MP RGB sensor.

- Upward-facing Sunshine Sensor for accurate imagery, whatever the light conditions.

- Customised data capture: capture multispectral data, RGB or both and chose its resolution.

- GPS system for the georeferencing of the captures photo with the geographic coordinate system.

---

[2] reference: www.senseFly.com
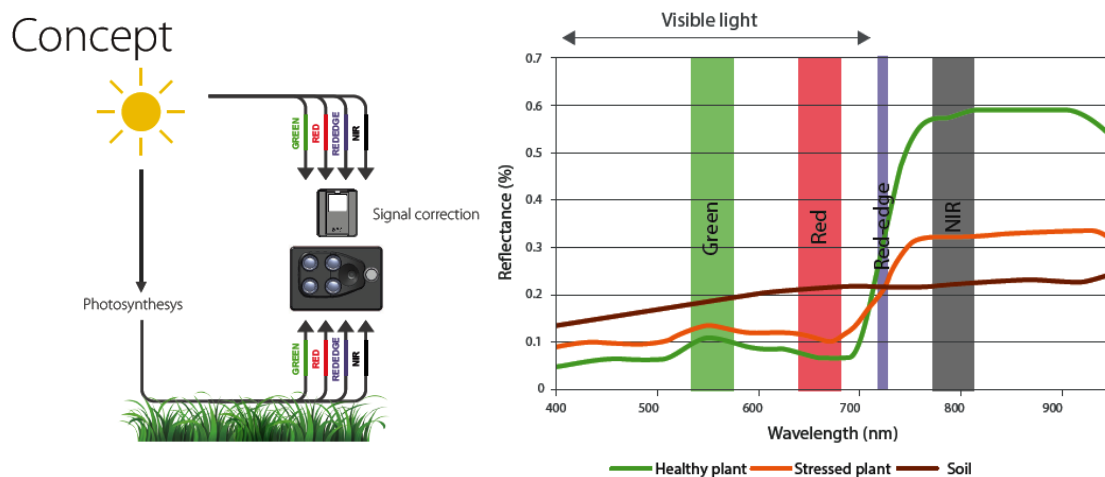
*Fig. 3 Concept and Vegetation reflectance*

The main idea is using the four multispectral sensors together with the sunshine sensor provide a reflectance measurement (Fig. 3) useful to analyse the amount of light captured and reflected (Fig. 4) from the plants and to evaluate the crop's health status in order to let the farmers make the best choice for their fields.
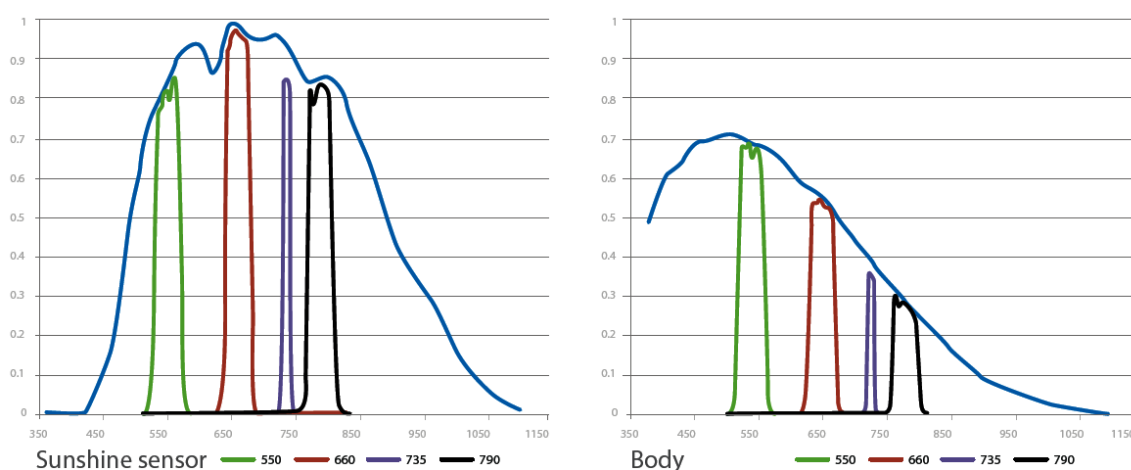


*Fig. 4 Parrot Sequoia Camera Sensitivity*

# 3. Photo Shots by RPAS

This process is structured in two phases, one concerns the planning of a flight mission and the second one in which the drone takes aerial photos.

## 3.1. Flight Mission planning

Through the proprietary software, called eMotion Ag, the mission is planned. To plan the flight, under the "Mission" panel, some fundamentals parameters have to be set.

- **"Briefing" tab**
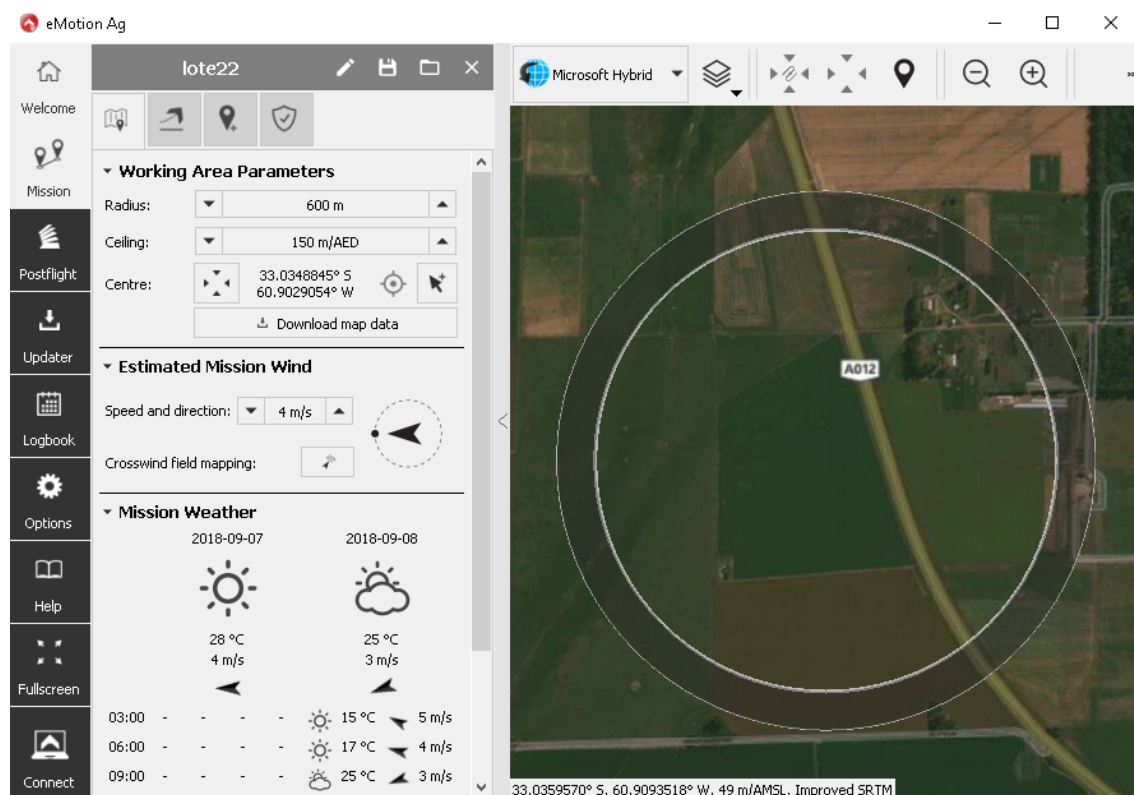


*Fig. 5 eMotion "Briefing" tab*

**Working Area Parameters:**

– <u>Radius</u>: it is the drone working area. This parameter is useful to coordinate the aerial traffic in order to not overlap with other aircraft flight (it's currently not working in South America area).

– <u>Ceiling</u>: it is the maximum height the eBee can reach during the flight.

**Estimated Mission Wind:**

– <u>Speed and Direction</u>: this is an important parameter because depending on the wind and speed direction the RPAS orientate itself. The eBee SQ flight concept is to take advantage of the wind to plane minimaxing the motor rotation and so save battery. To performs this the wind has to hit the drone in a transversal way as much as possible.

As well as high speed wind, as wind gusts, even week wind can affect in a significant manner, the success of the photo shots. The optimal conditions should be in a wind speed between 1-3 m/s, without wind gusts and without changing in wind direction.

- **"Take-off and landing" tab**
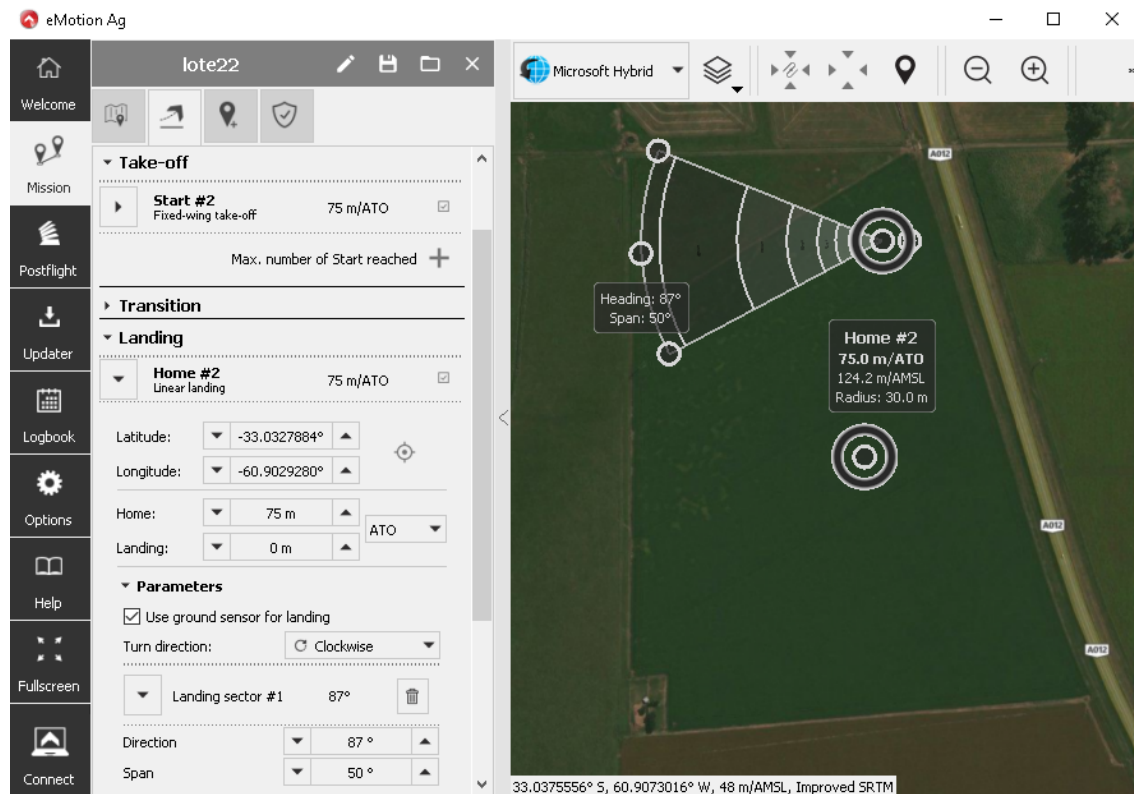


*Fig. 6 eMotion "Take-off and landing" tab*

**Take-Off:**

&ndash; Here is possible to set the altitude and Starting point position.

**Landing:**

&ndash; As in the take-off, altitude and position of Home point can be set. Here we must pay attention to choose a point free of elements that can damage the UAV; usually it is chosen directly in the lot just before the flight.

&ndash; <u>Parameters</u>: direction and span angles are defined a priori accordingly to the wind direction. The eBee SQ has a built-in sensor able to detect the real wind speed and direction. It uses this information to position itself upwind during the landing stage and, for this reason, the span angle needs to be big enough.

- **"Field" tab**
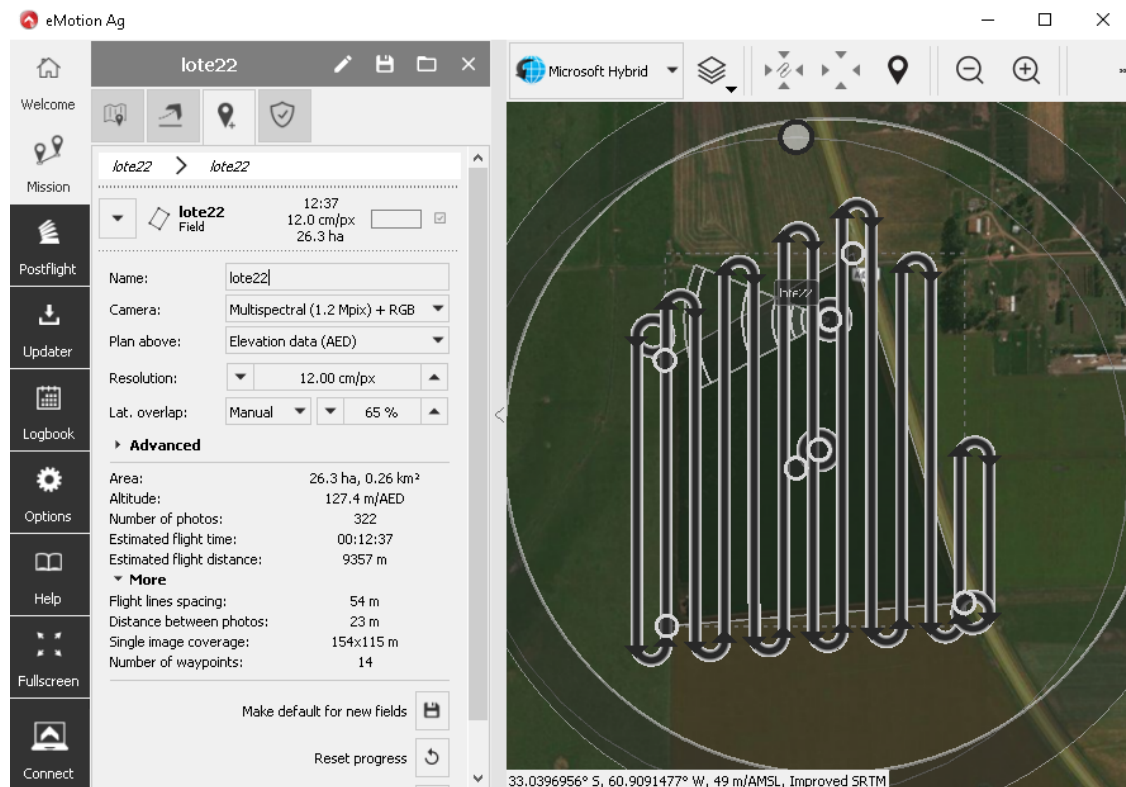


*Fig. 7 eMotion "Field" tab*

– Define the lot boundary.

– <u>Camera</u>: To choose with which kind of sensor take photos, multispectral and RGB or just one sensor. For our purpose we make use of the only multispectral camera.

– <u>Resolution and Lateral Overlap</u>: decreasing the value, cm/px, in the Resolution entry and increasing the value of Lat. overlap, we gain in photo's quality but in an exponential way increases the number of photos and the estimated flight time and distance. After some test, a good compromise is found, as shown above in the Fig. 7.

## 3.2. Photo Shooting Phase

Once the plan is realized and uploaded to the eBee SQ storage, the microprocessor can start to elaborate the info and so the drone can take-off and proceed to obtains pictures of the appropriate field.

There are some simple procedures before the flight can start. The first one is to link the UAV and PC, to allow the communication, by an USB Radio Modem (Fig. 8). The second one is to calibrate the Camera Sensors, referring to sunlight, with a calibration target (Fig. 9, it is essential to obtain accurate and truthful data from the sensors captures).



*Fig. 8 USB radio modem*



*Fig. 9 Calibration target*

During the mission a step by step flight progress of the eBee SQ drone is shown through the eMotion software (see Fig. 10). Some relevant information is displayed on the right panel which include Autonomy status (battery percentage,

flight time, wind speed and direction, etc.), Flight data (ground speed, altitude, gyroscope, coordinates, etc.), Instruments (camera and drone temperature, satellite info, etc.) and other less relevant data.
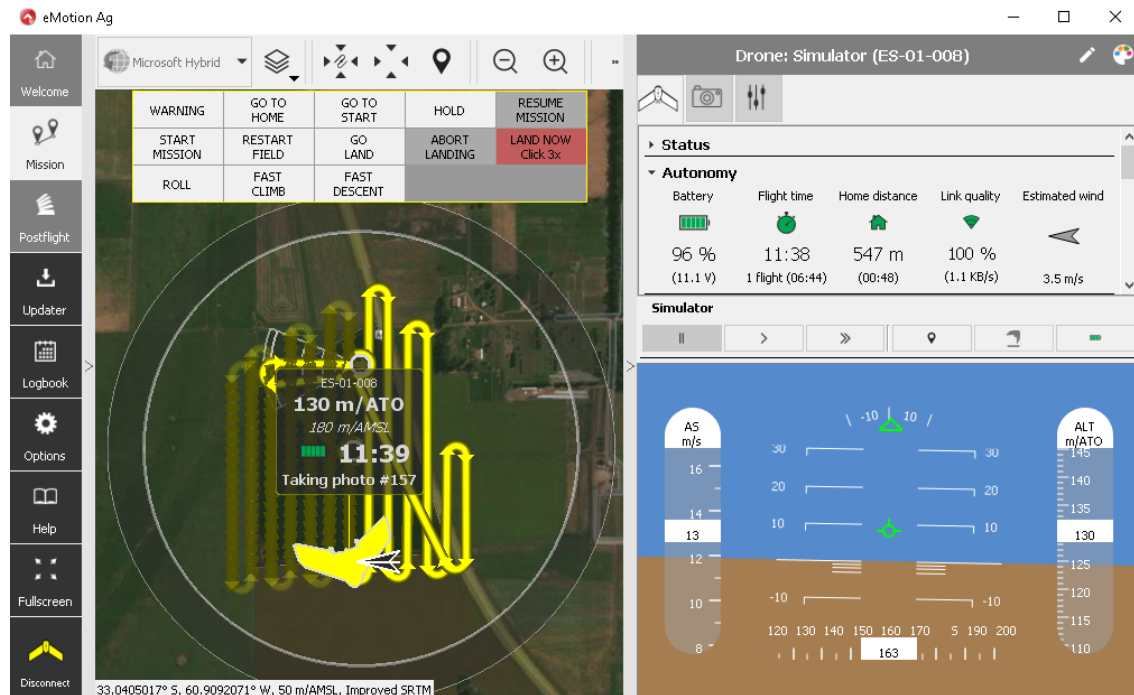


*Fig. 10 Flight and Photo Shoot step*



*Fig. 11 Take-off step*



*Fig. 12 Landing step*

Once the mission ends with success, to export the obtained photos, the eBee SQ is connected directly to the computer via USB.

Now under the "Postflight" panel, in the eMotion Ag software, a now project folder is created in which the flight logs and aerial photos will be downloaded from the UAV.

# 4. Post-flight photo processing

Now the pictures need to be elaborated in order to obtain a suitable data with which analyse the vegetation health status. To do this work a lot of software are available, one of the most powerful and well developed is the one we are going to use, and it's called Pix4Dmapper.

In the first chapter we are going to introduce the main software functionalities and next will follow an explanation about how the elaborated data are interpreted.

## 4.1. Pix4Dmapper introduction

Pix4Dmapper is a photogrammetry software and its main function is to turns drones captures into highly precise, georeferenced 2D maps and 3D models.

Opening the program to create a new project it asks to import the desired folder containing the photos, multispectral or RGB, previously downloaded from the drone, and to define which kind of project to create based on the type of image formatting.
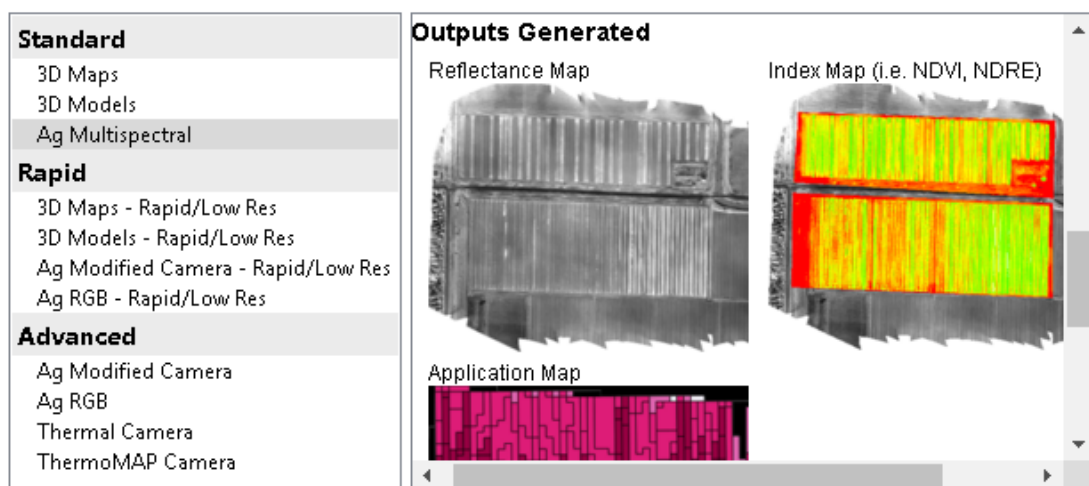


*Fig. 13 Pix4Dmapper "New project"*

The "Ag Multispectral" template generates as outputs three kinds of maps: Reflectance, Index and Application maps (see Fig. 13).

These aforementioned maps have a huge application fields as could be Digital scouting, Enhanced input management and Precision agriculture.

The first window, after the template selection, shows the map of the reference worked area with each point where the eBee SQ took the aerial photos.

Now the processing options can be personalized to meet our need. Some adjustments refer to Point Cloud and Mash or even on DSM (Digital Surface Model) and Orthomosaic and Index Calculator.

The term Point Cloud is used to describe a set of data points in a given space; a representation of a collection of multidimensional points. As our interests are on a 3D mesh, we focus on 3D point clouds as a collection of 3D points characterized by spatial XYZ-coordinates and may optionally be assigned additional attributes such as intensity information, thermal information, specific properties (e.g., in terms of orientation and scale), or any abstract information (e.g., vegetation indexes) (Rusu RB & Cousins S, 2011).

The DSM is the reconstruction of a 3D surface derived of the elaboration of the 3D point clouds. DSM captures the natural and built features and objects extrude from the Earth's surface. It is useful in many areas and in particular for vegetation managements to see how and where vegetation is encroaching.

## 4.2.  Pix4Dmapper – rayCloud –

Once the images are processed the Pix4Dmapper software shows, under the "rayCloud" panel, the DSM model where selecting any point of the surface or any aerial capture "satellite" is possible to visualize the different elements of the reconstruction (Camera Positions, Reprojections (rays), Processing Area, Point Cloud Densification and Classification, etc.) and their properties. Other options are: Verify/ improve the accuracy of the reconstruction of the model, georeference a project using GCPs and /or Scale and Orientation constraints, assign points of

the point cloud to different point groups, create objects and measure distances (polylines) and surfaces, export point cloud files using points belonging to one or several groups[3] (Fig. 14).
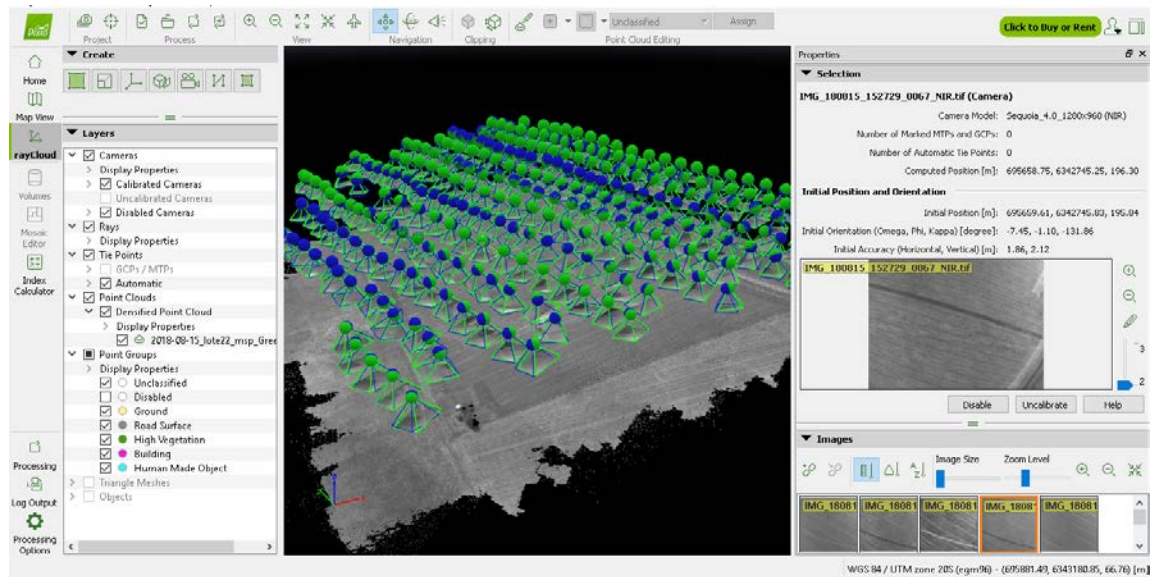


*Fig. 14 DSM surface*

## 4.3.  Pix4Dmapper – Index Calculator –

Calculate and index means to elaborate the data according some parameters defined by the index formula. There are a lot of indexes that can be used, each one has its functionality based on the application field.

Pix4Dmapper determines which Vegetation Index can calculate from the input data set. VI is used to detect the presence and relative abundance of various vegetation properties.

The software allows us to generate an Index Map where the colour of each pixel is computed using a formula that combines different bands of the Reflectance Map and so provide information about the bands of the Reflectance Map.

---

[3] reference: support.pix4d.com/hc/en-us/articles/202558639-Using-the-rayCloud

Talking about Reflectance Map we refer to the proportion of light reflected that a device can capture. The reflectance map is obtained from the DSM and is corrected for perspective. The value of each pixel is obtained as a weighted average of the pixels in the original images that correspond to this particular pixel. The weight of every pixel (from the original images) in the weighted average is also computed differently. The goal is to produce a map where the value of each pixel faithfully indicates the reflectance of the object[4].

In our Parrot Sequoia camera, we have four multispectral sensors (green, red, near-infrared, red-edge) so we obtain four different reflectance maps, one for each light band. The four light bands have different wavelengths and are respectively 550nm for green band, 790nm for near-infrared band, 660nm for red band, 735nm for red-edge band.

The main application of the reflectance maps is to visualize the Index Map as a coloured Index Map by applying a colour mapping to it. These colour bands define the classes of the Index Map to generate an Application Map[5].

Before we can calculate an index, it is necessary to generate the, previously mentioned, reflectance map and then draw the region of interest. It can be done in the "Index Calculator" panel, as shown in Fig. 15.

---

[4] reference: support.pix4d.com/hc/en-us/articles/202739409-Reflectance-map-vs-orthomosaic
[5] reference: support.pix4d.com/hc/en-us/articles/202558729-Using-the-Index-Calculator
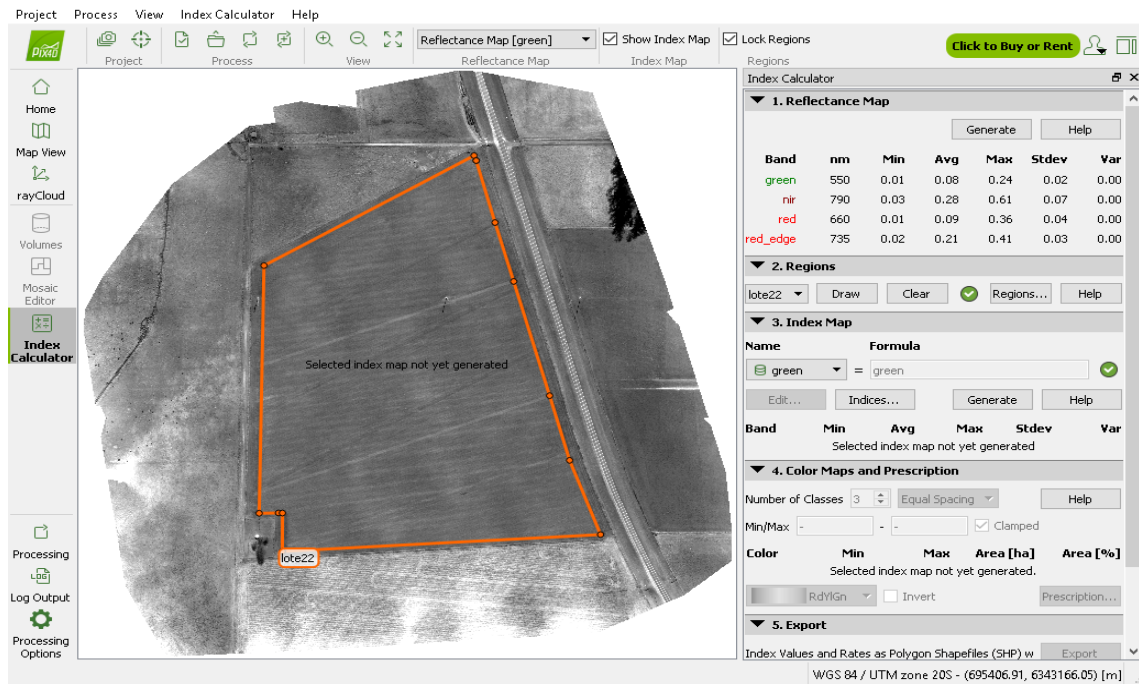
*Fig. 15 Reflectance Map*

Now it is finally possible to calculate any vegetation index combining the light bands of the reflectance map.

A Vegetation Index is a spectral calculation that is done between two or more bands of the source data designed to enhance the contribution of vegetation properties and allow for comparisons of photosynthetic activity across your area of interest.

When the VI calculation takes place, it goes pixel by pixel through your entire dataset and runs a calculation on the spectral values of that pixel. This will assign a value representing some version of plant health for each pixel in the image. These values are then generalized to different ranges and turned into the colorized map you see on screen when the calculation is complete.

VI's allow you to see relative differences in the general plant health across your entire field. Because these are relative differences in plant health across your field it is important to apply only to the areas you are interested in. For an example if you include a gravel road in the bounds of your vegetation index run the lower

side of your VI range is going to be thrown off by this non-living material included in your area of interest[6].

Applying VIs to vegetative materials to analyse their conditions does not produce absolute results. The results derived from the VIs are relative when determining where distribution or stress is, providing a theoretical level ranging from a low to high value.

We will make use of two Vegetation Index: NDVI and GNDVI.

NDVI (Normalized Difference Vegetation Index) is one of the oldest Vegetation Indexes out there. Most of the Indexes around are based from this original NDVI equation. This VI is a robust measure of healthy green vegetation.

The equation uses the highest absorption (Red Light) and reflectance (Green Light) waves of the visual spectrum to calculate the Vegetation Index value. It is a good indicator of chlorophyll content (Greenness) over a wide range of conditions. It can however saturate in dense vegetation conditions when Leaf Area in the survey becomes high.

$$NDVI = (NIR - Red) / (NIR + Red)$$

Values range from -1 to 1. Common range for green vegetation is 0.2-0.8 (Rouse J., R. Haas, J. Schell, and D. Deering, 1973).

GNDVI acronyms stand for Green Normalized Difference Vegetation Index and it is an index of greenness or photosynthetic activity of living plants. It is specifically sensitive to the variation of chlorophyll content in plants. You can see below this algorithm is also very similar NDVI with the substitution of Green instead of Red in the equation. Because of this change the GNDVI is more sensitive to the concentration of chlorophyll in plants.

$$GNDVI = (NIR - Green) / (NIR + Green)$$

---

[6] reference: support.precisionmapper.com/support/solutions/articles/6000187227-vegetation-indices-for-multispectral-data

If a plant is taking in the right amount of water or nitrogen it becomes greener and healthier. These elements fuel the photosynthesis process through the production of chlorophyll. Because of this the GNDVI algorithm is most commonly used to determine water and fertilizer uptake across a field. With good source data and GNDVI results you will be able to allocate your water and fertilizer in a more effective way (Gitelson A., and M. Merzlyak, 1998).

After this extensive introduction about VI, we can calculate the NDVI and GNDVI applied to our lot of interest. To do that, we proceed whit the built-in instrument of the Pix4Dmapper which proposes itself some VI based on the input sensors data, but it is also possible to create new ones introducing their relative formulas. After generating the abovementioned VI, the software returns as output an Index Map.

It is now possible to play with the Color Map defining the numbers of classes (numbers of colour band) and which kind of classification method (equal Spacing, equal Area or Jenks). The equal Spacing and Area methods are defined within the name descriptions, it means that all classes have the same range or represents the same area respectively. For what concern the Jenks method, it uses the Jenks natural breaks classification method is a data clustering method designed to determine the best arrangement of values into different classes. This is done by seeking to minimize each class's average deviation from the class mean, while maximizing each class's deviation from the means of the other groups. In other words, the method seeks to reduce the variance within classes and maximize the variance between classes (Jenks G. and McMaster R., 1967).

Three classes of colour band and Jenks classification method (it is almost identical to the equal Spacing method), is what we are going to adopt.

A special consideration has to be done with respect of the data and location acquisition period and which kind of crops are going to be cultivated. In our case the experimental plot is in Zavalla, Santa Fe, Argentina (30º 02' 02,4" S, 60º 53' 46,8" W) on the South Hemisphere and the reference crop is wheat. For the wheat,

the seeding period going from April to July (Winter) and the harvesting period is between October and January (Summer).

Two different data sampling are going to be analysed and compared, the first one on 15 August 2018 and the other one on 05 October 2018.

## 4.3.1. Data Collection of 15th August 2018

Now the two vegetation indexes, of the same field, are generated and compared to visualize the main differences.

The following pictures and tables show in detail the field features with respect to the two vegetation indices used: NDVI and GNDVI.

As said in the previous chapter, we work we three colour classes. Each colour band contain information about the band width, the amount of area occupied by such colour band. In addition, the user can add more information, for example a Rate value (relative to the quantity of input, fertilizers, seeds, water, etc. to supply per hectare) with the relative total Quantity or a Comment for example to specify to which vegetation health status correspond that colour group.

Further the 'Pix4dmapper' software will link those data to the map and make possible to export the coloured indexed data map (GeoTIFF and GeoJPG) or the Index Values and Rates as Polygon Shapefile with Grid.

The three colours define the vegetation healthiness. Going from RED to GREEN means higher photosynthetic activity of plants so less needs in terms of water and nutrition and larger chance to produce more and with higher quality. The grey area instead, is the one out of field boundary or that exceed the colour bands intervals so detected as non-productive area.
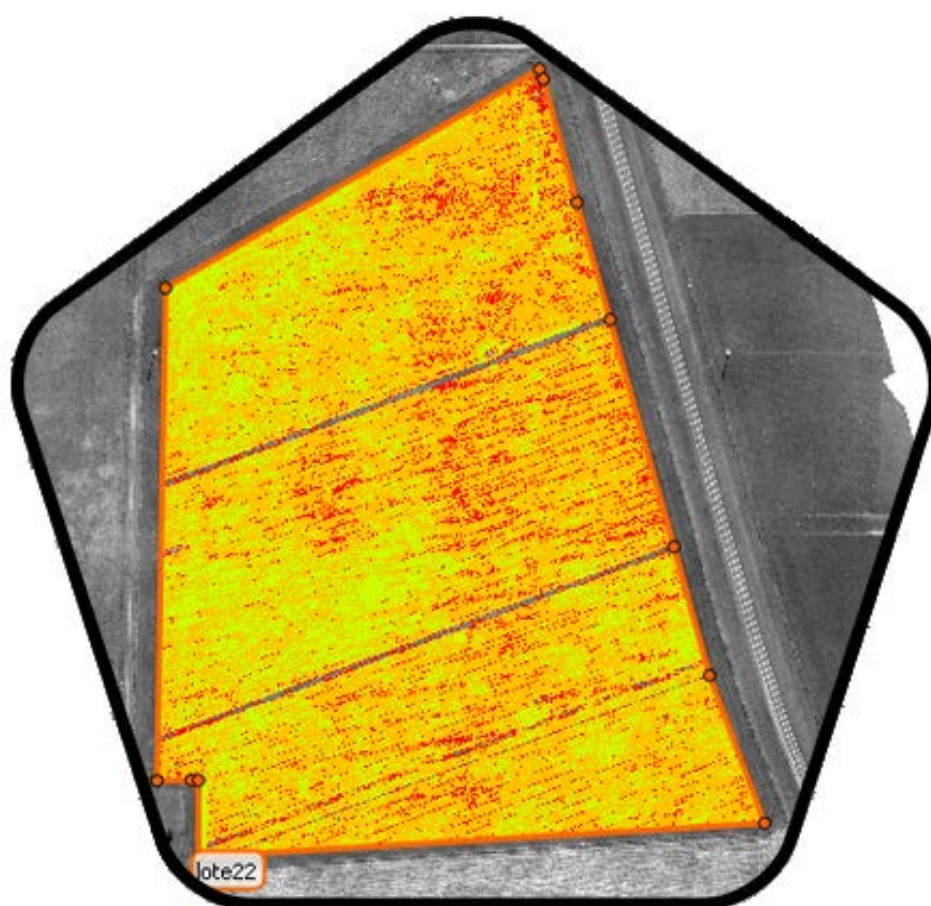
*Fig. 16 NDVI vegetation index*

| Colour | Min - Max | Area [ha] | Area [%] | Rate | Quantity | Comment |
|--------|-----------|-----------|----------|------|----------|---------|
|  | 0.73 – 0.89 | 4.69 | 23.58 | 10.00 | 46.90 | Healthiest |
|  | 0.58 – 0.73 | 13.07 | 65.74 | 20.00 | 261.49 | Moderate Stress |
|  | 0.43 – 0.58 | 2.12 | 10.68 | 0.00 | 0.00 | High Stress |
| **Total** | *0.43 – 0.89* | *19.88* | *100.00* | *30.00* | *308.39* | |

*Tab. 1 NDVI prescriptions*

The Fig. 16 and Tab. 1 show the NDVI Vegetation Index Map and its relative colour band prescription.
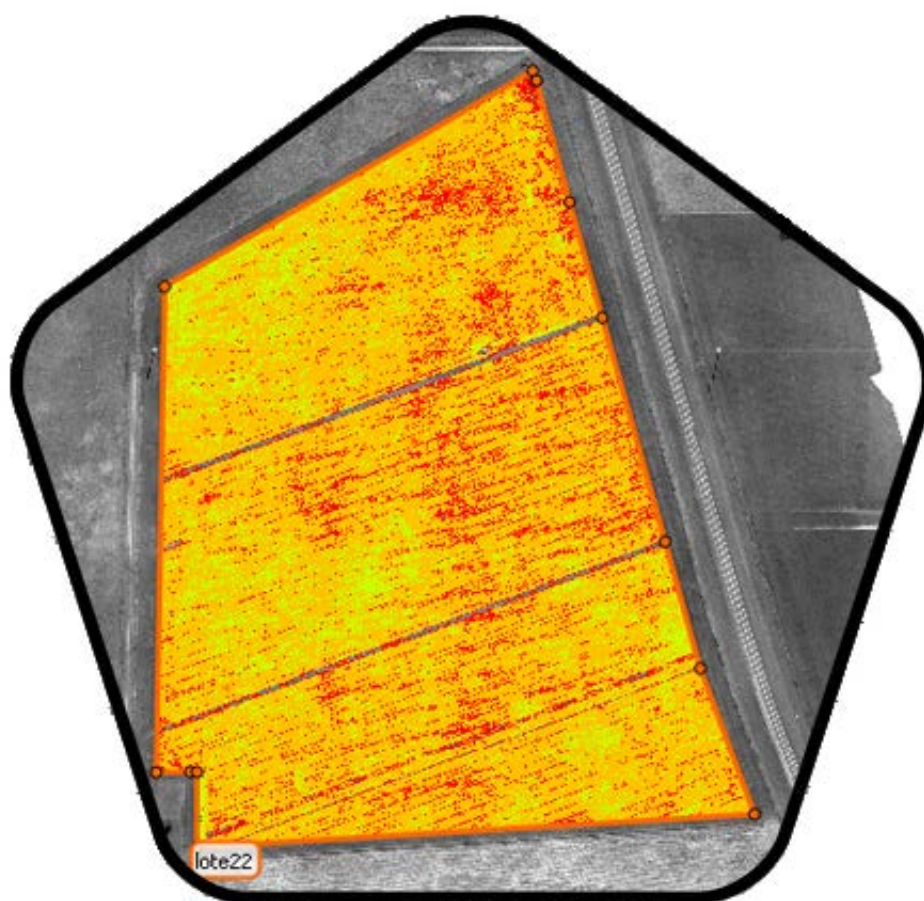
*Fig. 17 GNDVI vegetation index*

| Colour | Min - Max | Area [ha] | Area [%] | Rate | Quantity | Comment |
|---|---|---|---|---|---|---|
| | 0.68 – 0.77 | 2.56 | 12.88 | 10.00 | 25.61 | Healthiest |
| | 0.58 – 0.68 | 14.77 | 74.25 | 20.00 | 295.35 | Moderate Stress |
| | 0.49 – 0.58 | 2.56 | 12.87 | 0.00 | 0.00 | High Stress |
| **Total** | *0.49 – 0.77* | *19.89* | *100.00* | *30.00* | *320.96* | |

*Tab. 2 GNDVI prescriptions*

The Fig. 17 and Tab. 2 show the GNDVI Vegetation Index Map and its relative colour band prescription.
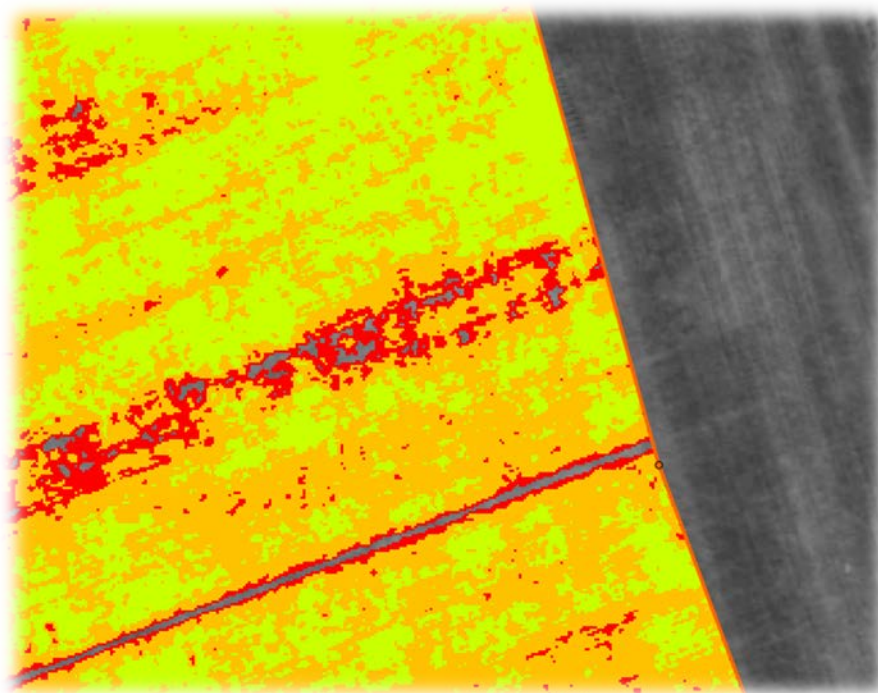
*Fig. 18 NDVI details*
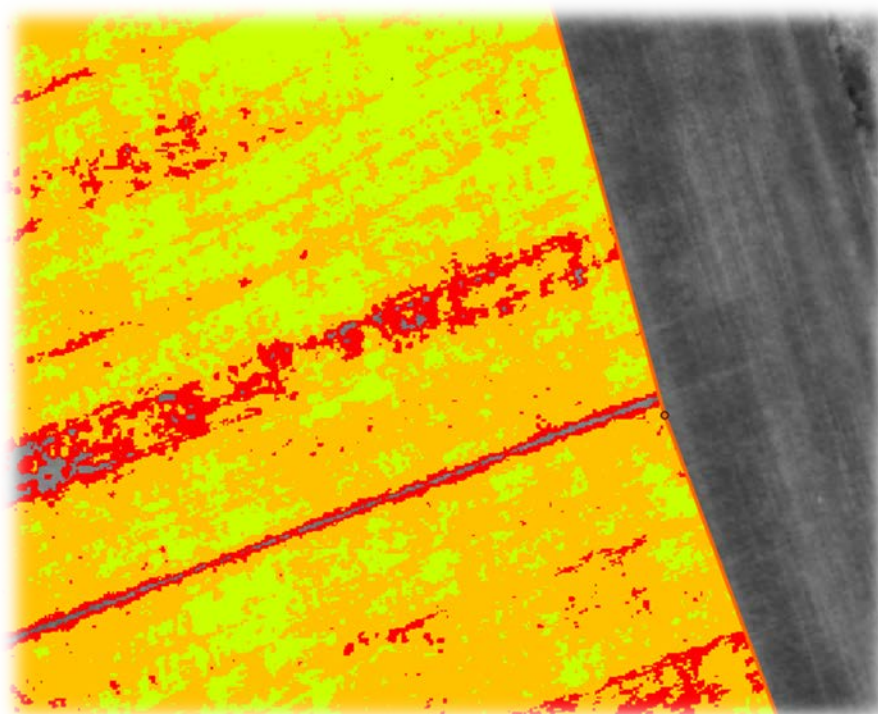


*Fig. 19 GNDVI details*

In the entire map pictures (Fig. 16 and Fig. 17) is difficult to appreciate the differences between the two vegetation indexes. These subtle differences,

instead, thanks to a zoom-in of the same field area, are appreciable both graphically (Fig. 18 and Fig. 19) and numerically (Tab. 1 and Tab. 2).

One first difference is that the NDVI has a wider index range, it means that each class is larger. Second, the area distribution changes within both VI: in the GNDVI we have a significant increase in the middle class, the Orange one, to the detriment of the Healthiest area, while the Red region changes a little. This is a quite important parameter because according to the type of class the treatment will be different in terms of quantity. For example, assuming to fertilize the parcel in this way: 10 kg/ha for the Green area, 20 kg/ha for the Orange area and no treats for the High Stressed area. Finally, as the GNDVI's orange area is wider than the NDVI's one, and considering the just mentioned treatment's rate, the total amount of needed fertilizers is higher in the Green Normalized Difference VI, from which derives that is higher also the cost of treatment.

As said the NDVI is an index useful principally to evaluate the vegetation density and the general health status of the crops. In the contrary the GNDVI returns values according to the chlorophyll concentration and thus the amount of water or nitrogen absorption. The Green Normalized Difference Vegetation Index is the one we are going to take greater in account because the final purpose of this project is to cure the yields in terms of the amount of water or fertilizers or herbicides to dispense depending on the needs.

## 4.3.2.    Data collection of 5th October 2018

To better analyse the real characteristics of the soil, another aerial expedition is realized. A date of October fifth is chosen because, after almost two months, the differences with the previous data sampling can be easily appreciated; moreover, the harvesting period is approaching and therefore the nutritional needs of the crop change.

As before, the following pictures (Fig. 20 and Fig. 21) and tables (Tab. 3 and Tab. 4) show the field characteristics respectively for  NDVI and GNDVI vegetation indexes.
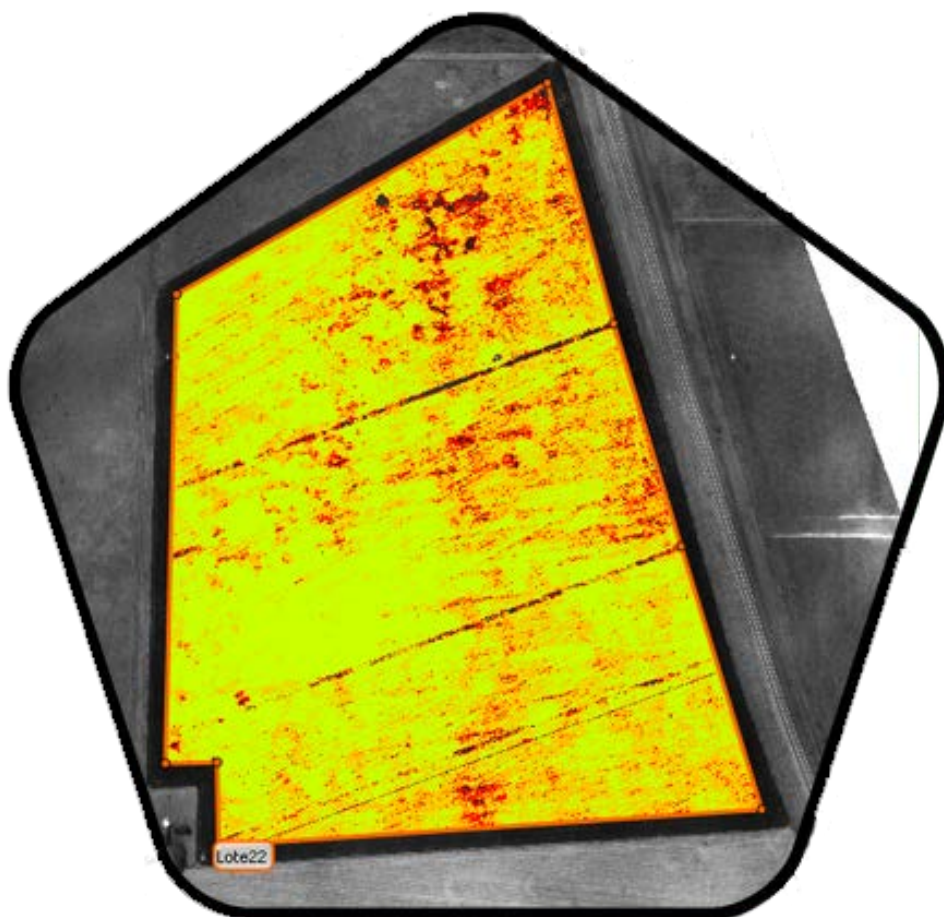
*Fig. 20 NDVI vegetation index*

| Colour | Min - Max | Area [ha] | Area [%] | Rate | Quantity | Comment |
|--------|-----------|-----------|----------|------|----------|---------|
| | 0.88 – 0.93 | 10.67 | 55.23 | 10.00 | 106.75 | Healthiest |
| | 0.84 – 0.88 | 7.50 | 38.78 | 20.00 | 149.91 | Moderate Stress |
| | 0.79 – 0.84 | 1.16 | 6.00 | 0.00 | 0.00 | High Stress |
| **Total** | *0.79 – 0.93* | *19.33* | *100.00* | *30.00* | *256.66* | |

*Tab. 3 NDVI prescription*
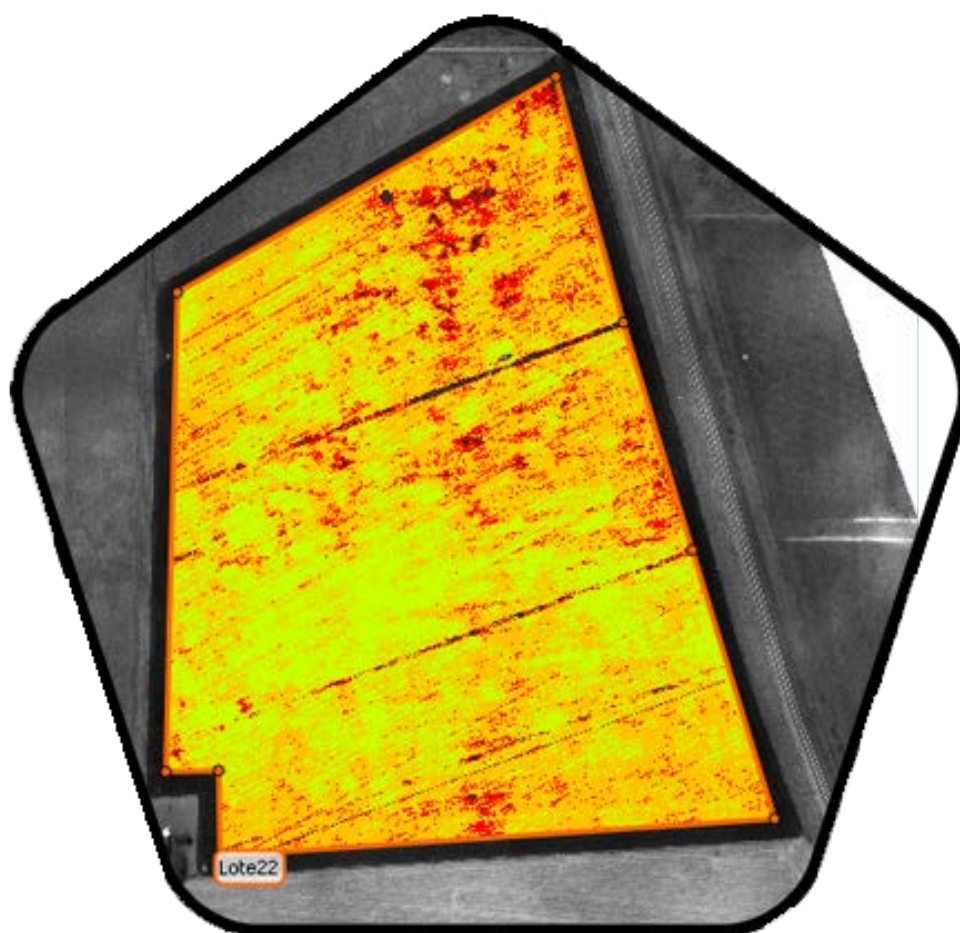
*Fig. 21 GNDVI vegetation index*

| Colour | Min - Max | Area [ha] | Area [%] | Rate | Quantity | Comment |
|---|---|---|---|---|---|---|
|  | 0.82 – 0.87 | 6.40 | 32.99 | 10.00 | 63.97 | Healthiest |
|  | 0.78 – 0.82 | 11.29 | 58.21 | 20.00 | 225.77 | Moderate Stress |
|  | 0.74 – 0.78 | 1.71 | 8.80 | 0.00 | 0.00 | High Stress |
| **Total** | *0.74 – 0.87* | *19.33* | *100.00* | *30.00* | *289.73* |  |

*Tab. 4 GNDVI prescription*

In Fig. 22 and Fig. 23, magnified a field region, the differences between the two vegetation indexes is very appreciable.
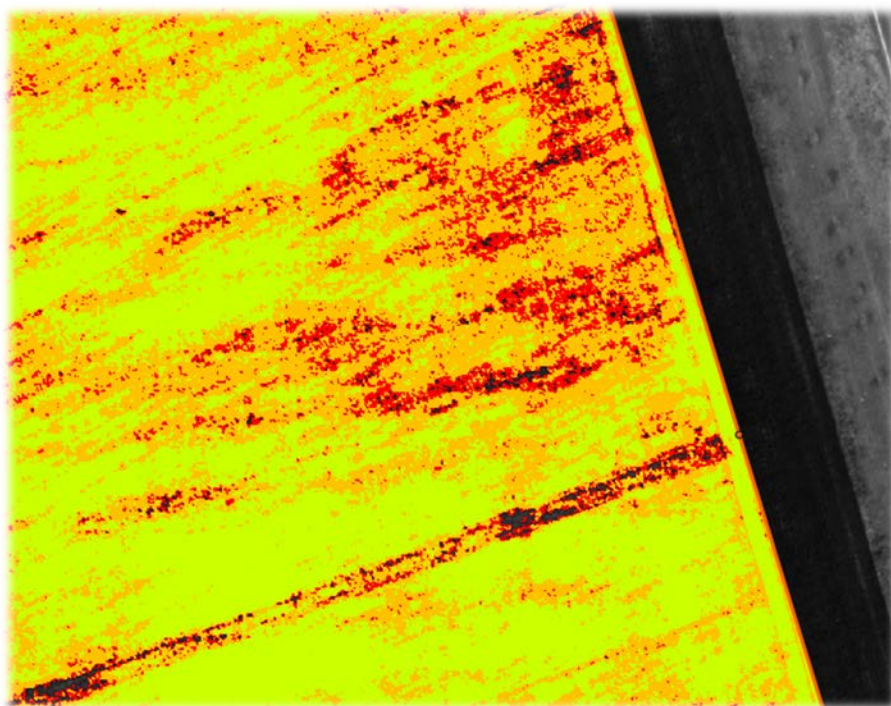
*Fig. 22 NDVI details*
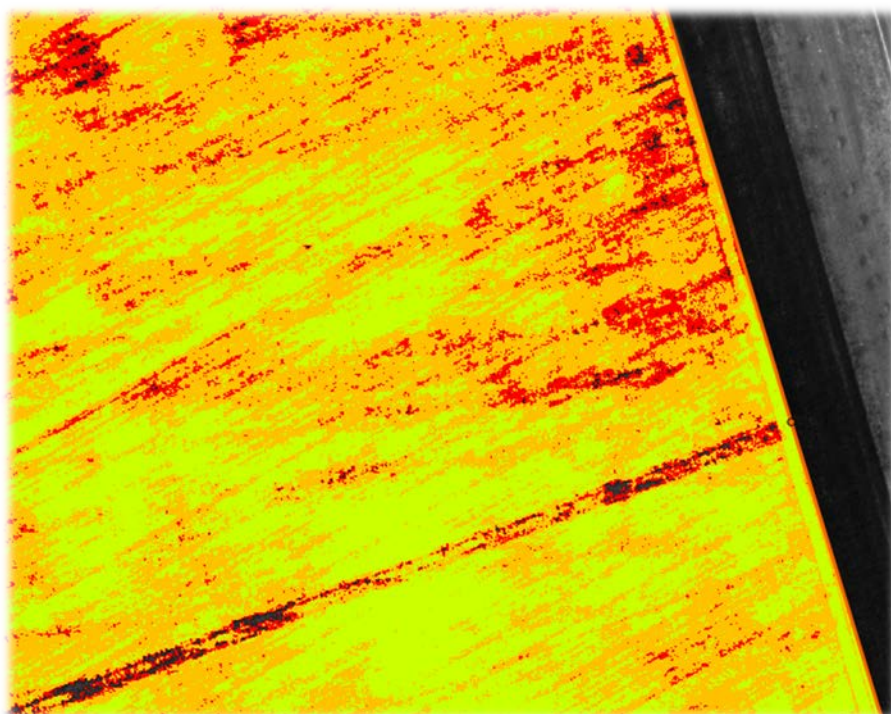


*Fig. 23 GNDVI details*

A clarification to do is that in this experimental field, for sake of study, any kind of treatment is carried out so no water, fertilizes or herbicides are supplied to the soil.

In this data collection, the differences between vegetation healthiness are better visible than August sampling. This because, while no treatment is executed, the strongest plants have grown better than weak ones. It results in a wider Green Area at the expense of Orange and Red ones.

Using the same Rate values as the first data sampling, actually the values should be lower as we are close to the harvesting period thus the plants have less power to synthesize nutrients, is possible to see how a reduced quantity of nutrients is needed, consequently to the fact that has significantly increased the amount of healthy plants (needs less supply); in this particular case about 20% and 10% less respectively for the NDVI and GNDVI indexes.

## 4.4. Soil Analysis

Deeper analysis to evaluate the soil characteristics can be performed studying the edaphic variables with different methods.

Those methods include techniques of Penetration, Infiltration and Structural Stability.

### 4.4.1. Standard Penetration Test

Penetration test is a procedure, used in the determination of the geotechnical characteristics of a terrain. The standard penetration test (SPT) (Fig. 24) consists in the introduction into the ground of a penetration element, generally of conical shape, joined together with a linkage.
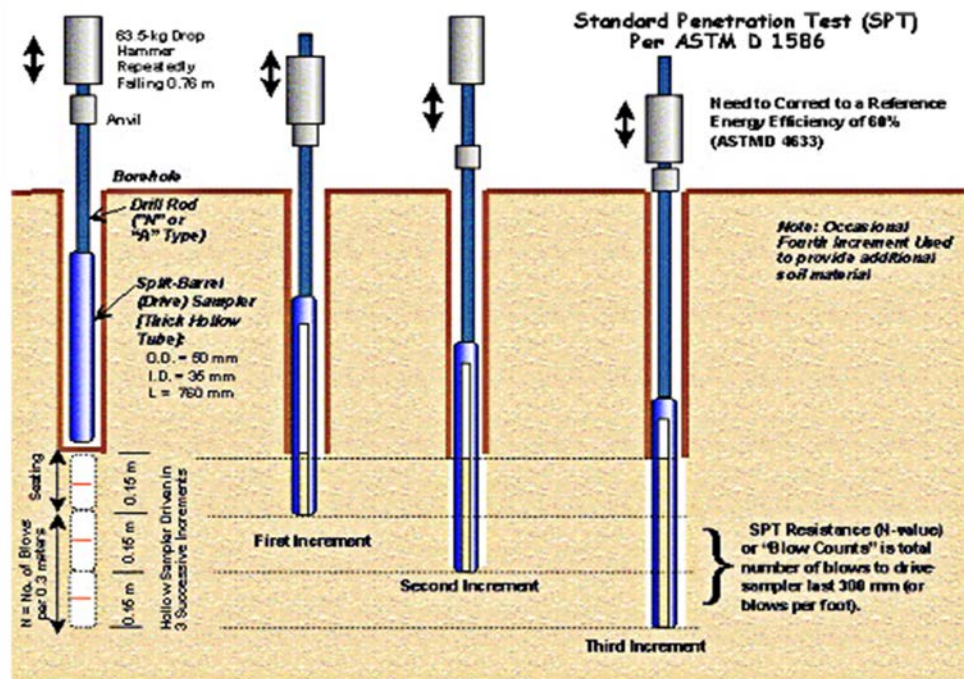
*Fig. 24 Standard Penetration Test*

The test procedure is described in ISO 22476-3. It uses a thick-walled sample tube, with an outside diameter of 50.8 mm and an inside diameter of 35 mm, and a length of around 650 mm. This is driven into the ground at the bottom of a borehole by blows from a slide hammer with a mass of 63.5 falling through a distance of 760 mm. The sample tube is driven 150 mm into the ground for three times until reaching 450 mm and then the number of blows needed for the second and third penetration, 150 mm each, is recorded. The sum of the number of blows required to penetrate from 150 mm to 450 mm is termed the "standard penetration resistance" or the "N-value". In cases where 50 blows are insufficient to advance it through a 150 mm interval the penetration after 50 blows is recorded. The blow count provides an indication of the density of the ground, and it is used in many empirical geotechnical engineering formulae.

| STP Density value | SPT N value | Bulk Density (kg/m³) |
|---|---|---|
| Very loose | 0 - 4 | < 1600 |
| Loose | 5 - 10 | 1530 - 2000 |
| Medium | 11 - 30 | 1750 - 2100 |
| Dense | 31 - 50 | 1750 - 2245 |
| Very Dense | > 50 | > 2100 |

*Tab. 5 STP Density Value*

The United State Department of Agriculture (USDA) defines bulk density as an indicator of soil compaction and soil health. It is the weight of dry soil per unit of volume typically expressed in grams/cm3. It affects infiltration, rooting depth/restrictions, available water capacity, soil porosity, plant nutrient availability, and soil microorganism activity, which influence key soil processes and productivity. Total volume of surface soil is about 50% solids, mostly soil particles (45%), and organic matter (generally < 5%); and about 50% pore space which are filled with air or water (Fig. 25).
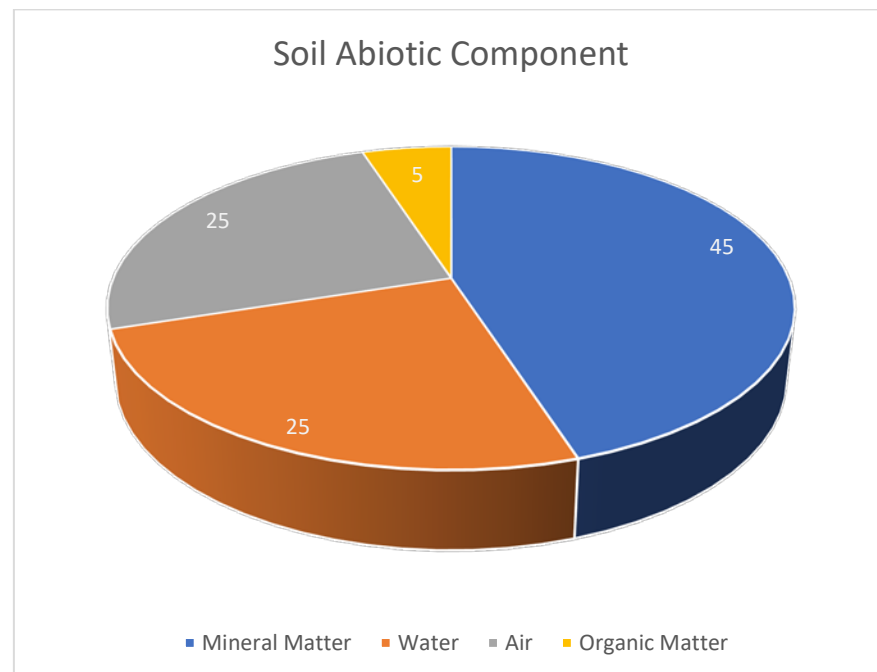


*Fig. 25 Abiotic Soil Components*

When determining bulk density, the amount of soil moisture must be determined. Available water capacity is the amount of soil moisture available to plants, varies by texture (Fig. 26), and is reduced when compaction occurs.
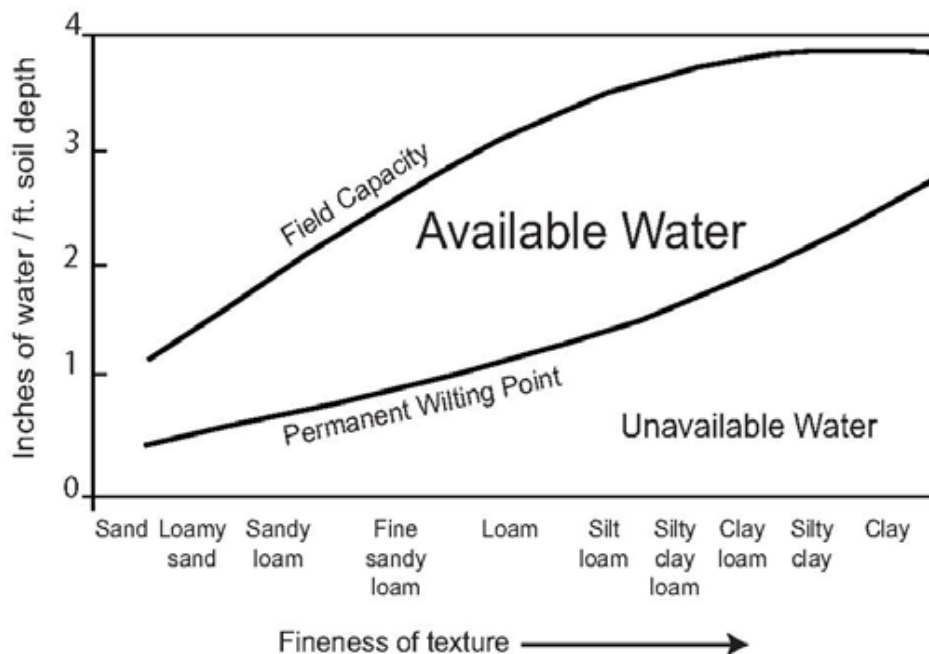


*Fig. 26 Available Water capacity*

Bulk density can be managed, using measures that limit compaction and build soil organic matter.

High bulk density is an indicator of low soil porosity and soil compaction. It may cause restrictions to root growth, and poor movement of air and water through the soil. Compaction can result in shallow plant rooting and poor plant growth, influencing crop yield and reducing vegetative cover available to protect soil from erosion. By reducing water infiltration into the soil, compaction can lead to increased runoff and erosion from sloping land or waterlogged soils in flatter areas. In general, some soil compaction to restrict water movement through the soil profile is beneficial under arid conditions, but under humid conditions compaction decreases yields.

In the agricultural department of the Rosario National University various SPT have been carried out in different points of the examined field; these points are shown in Fig. 27.
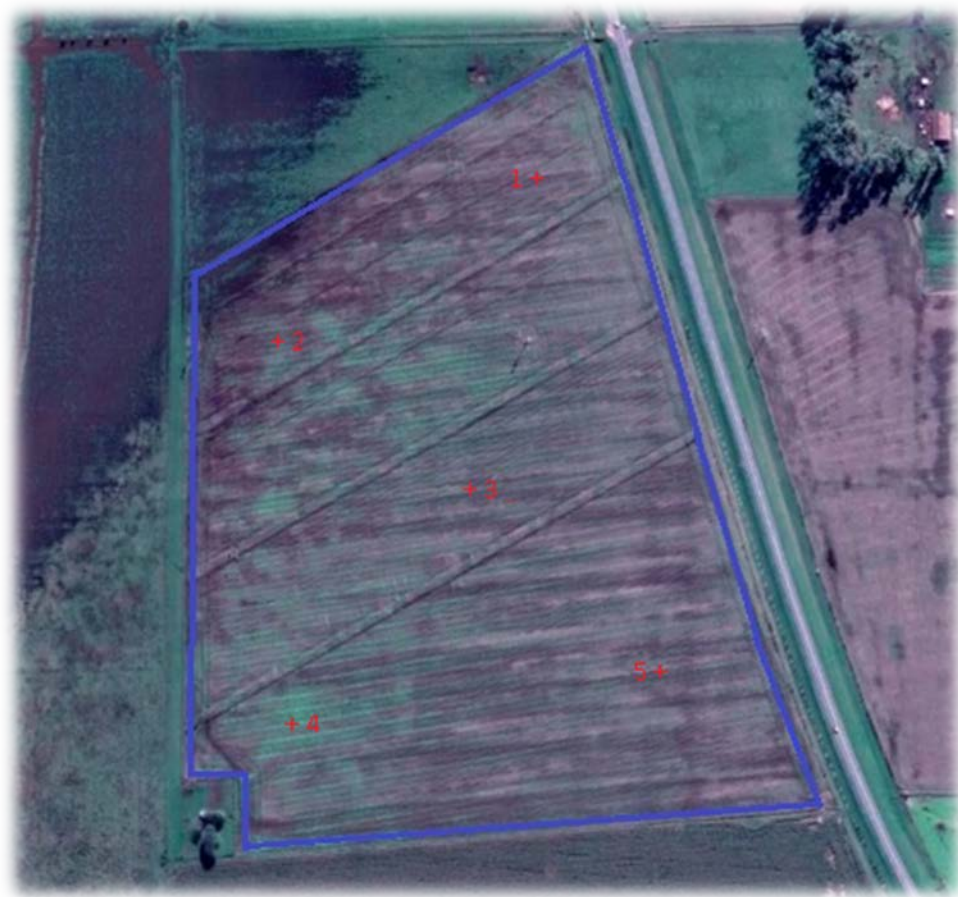
*Fig. 27 SPT penetration points*

From the investigations it emerges that the N-value range vary between 22 and 34, specifically:

|         | Point 1 | Point 2 | Point 3 | Point 4 | Point 5 |
|---------|---------|---------|---------|---------|---------|
| N-value | 25      | 31      | 30      | 34      | 22      |

*Tab. 6 SPT N values*

These values partly explain why in points 1, 3 and 5 the vegetation is less thick because the soil is less dense than in points 2 and 4 where the soil is more compact and therefore with a greater water retention capacity.

We recall that normally in the case of a climate rich in rainfall, or with a water source availability, a compact soil presents an unbalanced relationship between water and air, which would make the roots growth more difficult. While

this region of Argentina being slightly arid, and the irrigation practice is practically not used, a denser soil is preferable.

It was also found that at the lower density points, there is sometimes a slight ground relief while on the contrary, at high density, a slight ground depression is associate d and therefore a greater accumulation of water in case of precipitations.

## 4.4.2.    Infiltrometer Test

Infiltrometer test (Fig. 28) consists in the study of the hydraulic properties of the soil. It is based on obtaining the steady flow rate for long times. Commonly used infiltrometers are single-ring and double-ring infiltrometers.
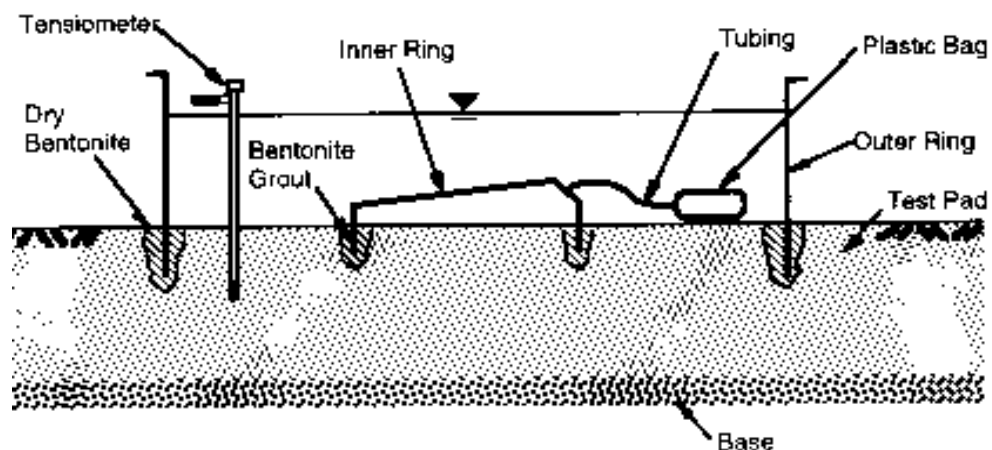


*Fig. 28 Double-Ring Infiltrometer test*

## 4.4.3.    Structural Stability Test

Structural Stability stands for the arrangement and organization of the soil constituent particles (Fig. 29). Such particles in their state of maximum division constitute discrete particles, which are approximately indivisible by the forces of the water of irrigation and the tensions that are generated during drying. The soil structure has influence on most of the growth factors of plants, being, in certain cases, a limiting factor in production.
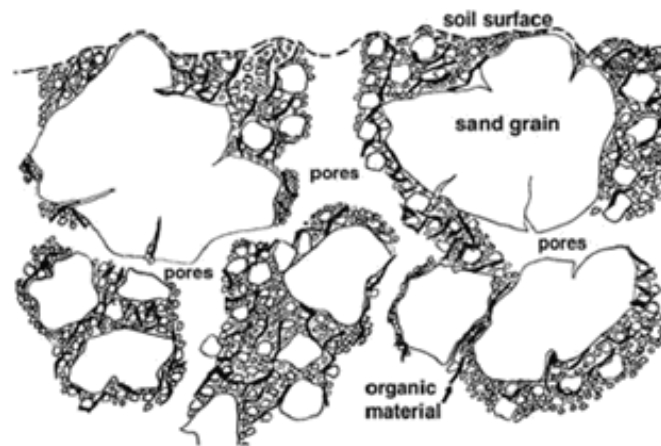
*Fig. 29 Soil structure*

Structural tests are carried out in 2012 by some students of the UNR, Bondaz C., Garbarino I., Lázzari J., relating to the lands of the city of Melinqué in the south of the province of Santa Fe, reveal the structural characteristics of the soil of that region, and thanks to the proximity to the Rosario department, even in our experimental field, the subsequent statements can be considered acceptable.
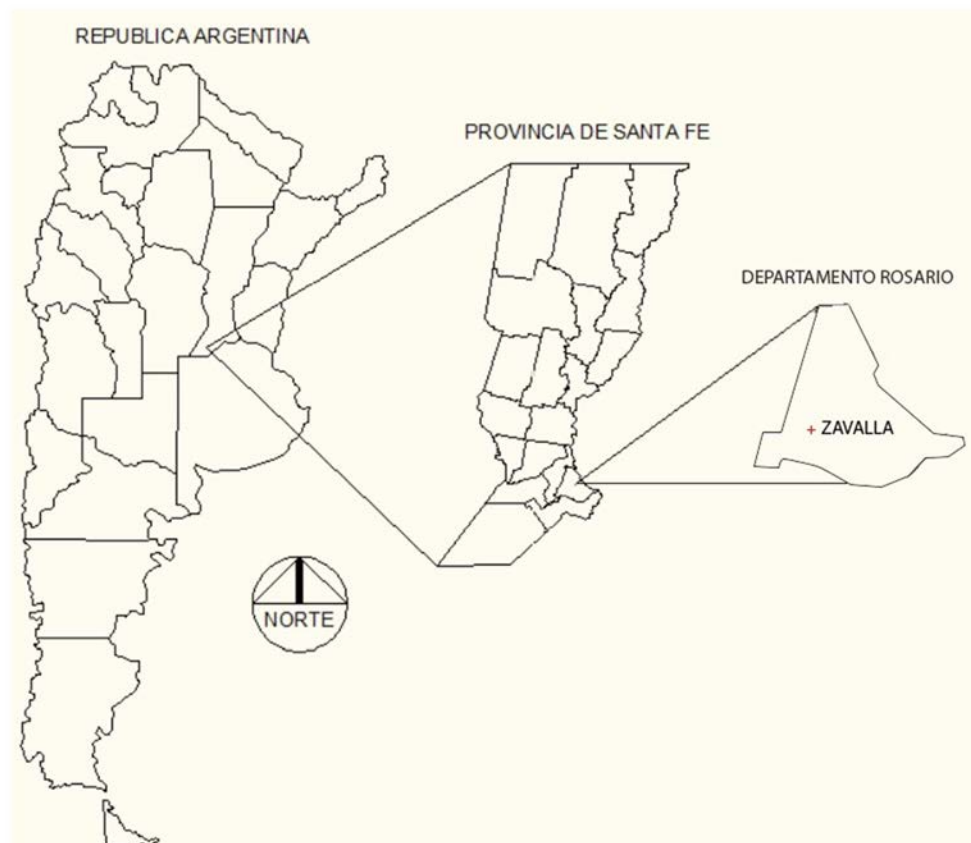


*Fig. 30 Experimental Field location*

"It is a dark and deep soil, with agricultural aptitude in a landscape of extended hills, with good drainage, it has developed from a loessic sediment of coarse loamy texture, not alkaline, not saline, with slopes that do not exceed 0 – 1 %"

**Taxonomic Classification**: Typically Agricultural, Fine, Mixed, Thermal Loam (USDA- S. Taxonomy V. 2006).

**Typical Profile Description**: 6/1075 C. Location 3360-31-1, Hughes

| | |
|---|---|
| A | 0 – 21 cm; dark greyish brown (10YR 3/2) wet; silty loam; moderate angular and subangular blocks; slightly hard; friable; slightly plastic; soft lower limit. |
| Bat | 21 – 33 cm; dark brown (10YR 3/3) wet; silty clay loam; moderately irregular prisms that break in moderate subangular blocks; friable; slightly plastic; slightly adhesive; abundant fine coating ("clay skins"); smooth lower limit. |
| Bt1 | 33 – 51 cm.; brown to dark brown (75YR 4/2) wet; silty clay loam; moderately irregular prisms that break into fine irregular prisms and into moderately angular blocks; friable; plastic, adhesive; abundant fine coating ("clay skins") of dark brown color; gradual lower limit. |
| Bt2 | 51 – 82 cm; dark brown to brown (75YR 4/3) wet; silty clay loam; moderately irregular prisms that break into irregular prisms and moderately angular blocks; firm; plastic, adhesive; very abundant medium coating ("clay skins") of dark brown color; regular lower limit. |
| BC | 82 – 103 cm; brown to dark brown (75YR 4/4) wet; silty to silty clay loam; weak medium irregular prisms that break into moderate subangular blocks; friable; slightly plastic; slightly adhesive; thin coating ("clay skins") of dark brown colour , weakly cemented at 10% of the volume of the horizon; gradual lower limit. |

*Tab. 7 Horizons Description*

**Profile location:** Latitude S 33° 45' 40'' y Longitude W 61° 22' 30''. Altitude 99 mAMSL to 6 km from Hughes North-West, General López department, Santa Fe province.

**Characteristic variability:** The thicknesses of horizons A and Bat vary, the latter with clay contents that can reach 40%. In some profiles a powdery calcareous horizon may appear with slight cementation.

**Phases:** By different degrees of erosion, slope and drainage are described in the cartographic units.

**Similar series:** El Arbolito, Rojas.

**Associate soils:** El Arbolito and La Sofía.

**Geographical distribution:** West from Colón, Buenos Aires province and North-Est from General López dept., Hughes district, Melincué and Carreras, de Santa Fe province. I.G.M. 3360-33-1 and 2; 3360-34-1 and 3360-27 and 28.

**Drainage and permeability:** medium drainage, moderate permeability with a deep-water table.

**Use and vegetation:** maize stover (Zea mays L.)

**Usability:** Class I-1 (USDA Soil Usability Class)

**Usability limits:** no limits.

**Productivity index by climate region:** 100 (A)

**Diagnostic features:** Mollisol, Udicic moisture regime, argillic horizon.

**Analytic Data:**

| | HORIZONS | | | | | | |
|---|---|---|---|---|---|---|---|
| | **A** | **Bat** | **Bt1** | **Bt2** | **BC** | **C** | **Ck** |
| **Depth (cm)** | 5-15 | 21-33 | 35-50 | 53-65 | 85-95 | 145-165 | 220-240 |
| **Organic matter (%)** | 3,46 | 1,50 | 0,86 | 0,53 | NA | NA | NA |
| **Total Carbon (%)** | 2,01 | 0,87 | 0,50 | 0,50 | 0,31 | 0,10 | NA |
| **Nitrogen (%)** | 0,174 | 0,097 | 0,072 | 0,069 | 0,047 | NA | NA |
| **C/N ratio** | 11 | 9 | 7 | 7 | NA | NA | NA |
| **Clay < 2 μ (%)** | 24,2 | 29,0 | 34,9 | 31,7 | 26,8 | 18,4 | 66,2 |
| **Silt 2-20 μ (%)** | - | - | - | - | - | - | - |
| **Silt 2-50 μ (%)** | 63,4 | 56,8 | 52,3 | 52,8 | 55,6 | 62,2 | 51,5 |
| **VFS 50-75 μ (%)** | - | - | - | - | - | - | - |
| **VFS 75-100 μ (%)** | - | - | - | - | - | - | - |
| **VFS 50-100 μ (%)** | 11,6 | 13,2 | 12,4 | 14,9 | 16,3 | 17,7 | 25,7 |

| | | | | | | | |
|---|---|---|---|---|---|---|---|
| **FS 100-250 µ (%)** | 0,8 | 1,4 | 0,4 | 0,6 | 1,3 | 1,7 | 2,4 |
| **MS 250-500 µ (%)** | - | - | - | - | - | - | - |
| **CS 500-1000 µ (%)** | - | - | - | - | - | - | - |
| **VCS 1-2 mm (%)** | - | - | - | - | - | - | - |
| **Calcareous (%)** | 0,0 | 0,0 | 0,0 | 0,0 | 0,0 | 0,0 | 4,2 |
| **Eq. humidity (%)** | 29,3 | 28,9 | 30,8 | 32,4 | 29,2 | 22,1 | 21,8 |
| **Paste resistance (Ω)** | - | - | - | - | - | - | - |
| **Conductivity (mS/cm)** | - | - | - | - | - | - | - |
| **Paste pH** | 6,2 | 6,1 | 6,4 | 6,2 | 6,3 | 6,6 | 8,0 |
| **pH H2O 1:2,5** | 7,5 | 7,5 | 7,3 | 7,6 | 7,6 | 7,7 | 8,5 |
| **pH KCl 1:2,5** | - | - | - | - | - | - | - |
| **EXCHANGE CATIONS** | | | | | | | |
| **Ca++ meq/100gr** | 11,6 | 10,6 | 12,6 | 14,6 | 13,6 | 9,8 | NA |
| **Mg++ meq/100gr** | 3,2 | 4,1 | 5,0 | 5,7 | 5,1 | 5,4 | NA |
| **Na+ meq/100gr** | 0,3 | 0,3 | 0,3 | 0,3 | 0,2 | 0,4 | 0,3 |
| **K meq/100gr** | 2,0 | 1,8 | 2,0 | 2,0 | 2,3 | 2,4 | 2,3 |
| **H meq/100gr** | 6,7 | 5,3 | 5,0 | 5,5 | 4,7 | 3,0 | NA |
| **CEC meq/100gr** | 20,3 | 21,0 | 23,7 | 26,3 | 24,0 | 19,3 | 16,6 |
| **Base saturation (%)** | 85 | 80 | 84 | 86 | 88 | 94 | NA |

NA: Not Analysed – VFS: Very Fine Sand – FS: Fine Sand – MS: Medium Sand – CS: Coarse Sand – VCS: Very Coarse Sand – meq: milliequivalent – CEC: Cation-Exchange Capacity

*Tab. 8 Analytic Soil Data*

### 4.4.4.    Conclusions

Soil analysis allows to validate the data obtained from drone photos and from vegetation indices and therefore how effectively a "green" area of the VI corresponds to a region with a greater Bulk density and vice versa for the areas of the "red" VI.

Those methods, along with the vegetation indexes and soil profile cartography, can help to know the plants real-needs and then adopt an adequate tillage operation to both increase the crop productivity and, at the same time, reduce the waste in time and supply.

# 5.  Path Planning Algorithm

## 5.1.  Introduction

The first thought on planning the algorithm was about to the kinematics of field machine. The kinematics studies the motion of points or objects without considering the forces that cause the motion (Thomas Wallace Wright, 1896).

Exist different coverage path planning (CPP) algorithms for the holonomic machine (can turns in place). However, most of farming machines are non-holonomic, and this increase the difficulty of planning cover path algorithms. There is no universal algorithm to solve this problem in non-holonomic situation so different solution are carried out.

Therefore, an important aspect to be investigated are the turning of a vehicle when searching for an optimal solution. The optimization consists in minimizing the time spent in each turn and its number. The efficiency of a route affects the energy consumption and the time needed to work the plot.

In most cases the planning of a route includes many more things than just optimal path. For example, a machine cannot carry more than a certain quantity of product, be it a fertilizer or a crop, so the machine must be regularly refilled or emptied. This element must be taken into consideration because it significantly affects the path planning.

During the years the so-called auto-guidance devices have become more common in agricultural field machines. These devices, thanks to the implementation of a GPS, help to keeps automatically the vehicle on-lane based on accurate satellite positioning.

Around the World an increasing number of autonomous machines without a driver are being developed, manly prototypes for research purpose but in the last few years some kinds of field robots are becoming commercials.

The main difficulties that delay the marketing of these products are mainly linked to a legislative, political and economic domain. Surely, the future of farming goes to this direction.

## 5.2. Field Analysis

Two considerations are analysed. The fields can be simply shaped, more or less, as square, rectangular or trapezoidal shape or could have an irregular shape due to some natural boundaries such as forests, rivers, etc. and can easily include obstacles.

As Argentina is an endless flat region, with a low-density population, so the cultivated plots are typically wide flat and regularly shaped without obstacles.

There are some regions of the world not so lucky, so the path planning is quite complicated. Thus, the path planning is more complicated and a feasible way to solve the problem is dividing it in simplest sub-problems.

The field plot is considered as 2D region, called polygon. A polygon is any 2D closed shape formed with straight lines or edges (Yuanxin Yang Alcocer) where the point in which two lines meet is called vertex. A simple polygon is a polygon where the edges not intersect with each other.

Exist various shape indexes and parameters are used to analyse the shape field. Within these, to remember, there are the convexity, the compactness, the regularity, the triangularity, the ellipticity, trapezoidality etc. All these indexes are useful to classify the class of field shape and its operational efficiency (T. Oksanen, 2007).

## 5.3. Vehicle Turning

A fundamental element in the total field working process is the non-working time of the field machine and in particular it refers to the time spent in headland turning. The headland is the region surrounding the plot where the

tractor performs curves. Minimizing as much as possible this non-working time results in an optimization in time and cost.

Commonly a tractor with a towed tool is used to perform operations as fertilizing, seeding or harrowing. In Fig. 31 a towed fertilizer spreader is shown.



*Fig. 31 Tractor-trailer vehicle*

Usually Numerical algorithms for solving this kind of optimal control problems are solved offline because its demand high computational resources and require a computer with high performance.

The machine moves on a 2D-plane; therefore, it has a three degrees of freedom (DOF). The planning algorithms depend on these vehicle constraints as well as field geometry restrictions.

There are mainly three types of turning patterns used in tillage operations: C-type, X-type, and R-type, as shown in Fig. 32. The C-type turning pattern is defined by the turning radius, R, and a turning angle of 90°. This C-type pattern features continuous forward motion and avoids reverse movement. When the tractor reaches a location where it will make a 90° turn, the PTO (Power Take-Off) power is shut off, the tillage implement is raised (if needed), and the tractor turns. The tractor then moves forward to another point and makes another 90°

turn, forming a C-shaped curve. The tractor stops at the first turning point, moves backward, and turns again to begin a new swath parallel to the master line. Similar to the C-type pattern, the R-type and Ω-type turning pattern involves only forward motion. The X-type turning pattern consists of a combination of a straight line and two 90° turns (as well as Y-type). The Fishtail-type turning pattern consist on three 60° turns, two forward and one backward motion. The tractor makes a left turn and then a right turn and continues moving forward on an adjacent line (Seo, 2010).



*(a) C-type turning*

*(b) R-type turning*

*(c) Ω-type turning*

*(d) Fishtail-type turning*

*(d) X-type turning*
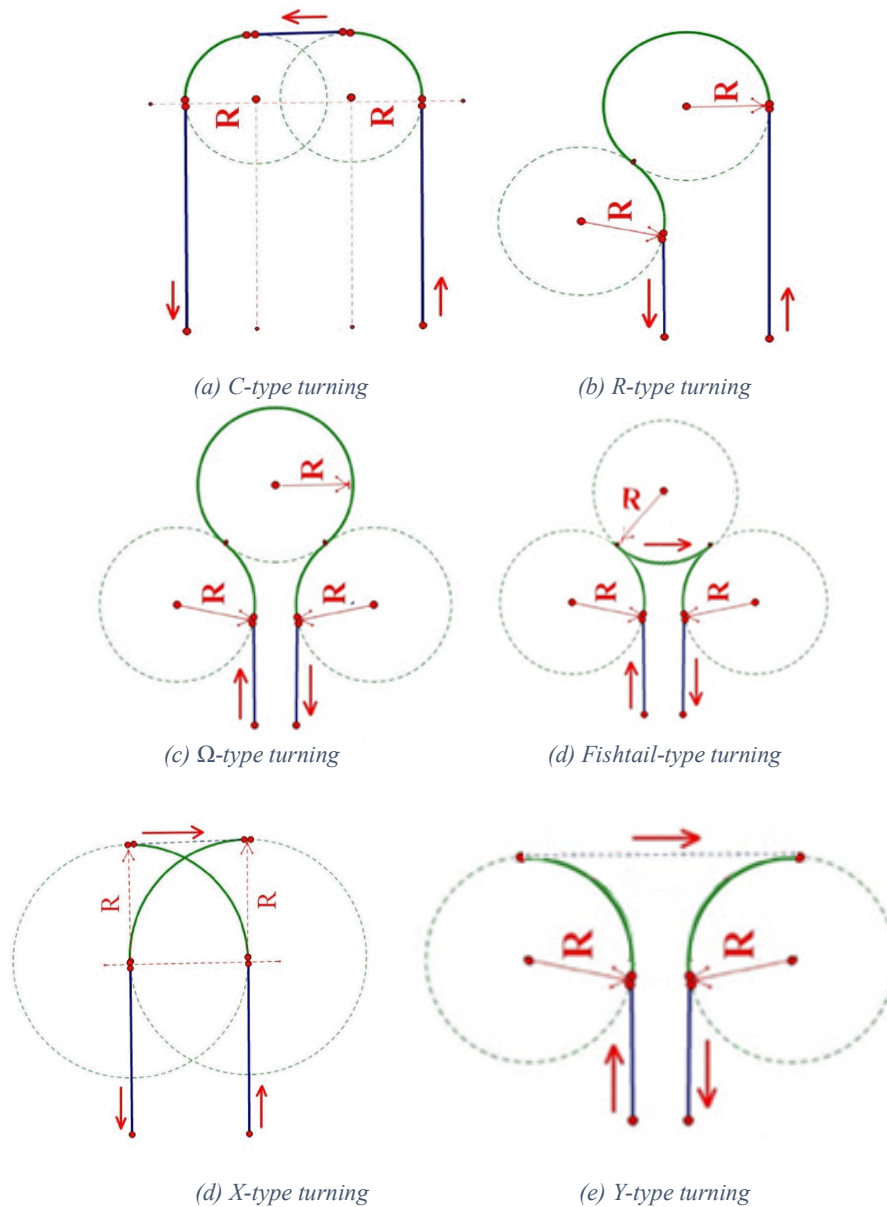
*(e) Y-type turning*

*Fig. 32 Turning Patterns*

The study on the type of curve is very important because it affects not only on a useless time spent but also on the occupied area to perform the turn; that area will be unproductive due to crop detriment caused by the machine movement. In Fig. 33 and Fig. 34 is shown an example of turns area not productively exploited.



*Fig. 33 Agricultural Machine turn*



*Fig. 34 Field R-type turns*

The evaluation on the type and the way to calculate the turning are about some tractor and plot parameters like tractor steering angles and headland width, working track width, etc (Fig. 35). For vehicle full automatized create an automatic turning pattern in headlands is important. The solution is to find the optimal trajectory in order to move the vehicle from a non-working position to the next working position in the shortest possible time and occupying the smallest possible area, so reducing the headland zone with the natural extension of productive region.



*Fig. 35 Field and Headland parameters*

Automatic turns creation in headlands is important if the field machines are fully automatized.

## 5.4.   Algorithm

### 5.4.1.     Path Planning Literature Review

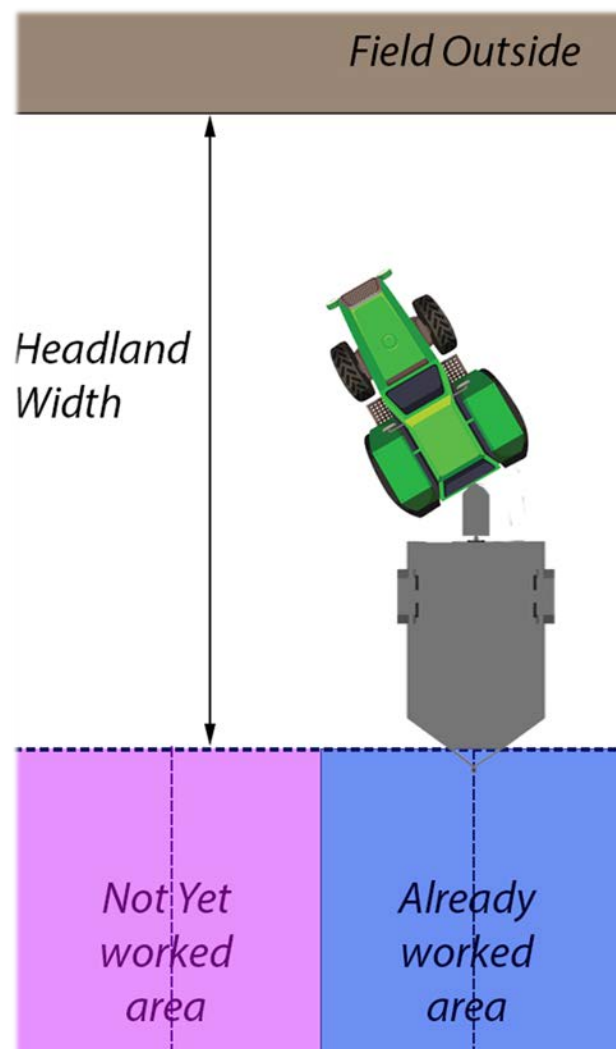An algorithm for path planning is based on the idea that the route includes a start and end points, avoids collisions with obstacles and the path is optimal according to some parameters such as time minimization.

In agriculture, the goal is not to move between two points, but to cover a whole field. For this reason, traditional route planning algorithms cannot be directly applied.

In robotics the route planning is subdivided into quantitative and qualitative navigation categories. In quantitative navigation, a series of information or maps, describe the environment with precision and the robot does not need any special tools to navigate. In qualitative navigation, on the other hand, the environment is not exactly known but it is structured in such a way that the robot can identify various reference points locate him to reach the end of the path; in this case the robot needs some more tools to know the environment (Murphy 2000).

An algorithm can be classified to be offline or online. Online algorithm does not need to know anything about what size it will processes as input in the beginning of the algorithm. It processes them piece by piece. Usually online algorithms perform real-time measurements based on sensor input and are needed if some kind of adaptivity to the environment is needed. In the other hand, an offline algorithm requires all information before the algorithm starts. To do that an exact knowing of the environment and the input size before the algorithm starts processing the data are needed. It should be noted that this thesis deals with the offline problem. In the following picture (Fig. 36) a robot path classification is presented, where the know environment is related to offline algorithms, while unknow environment concerns online algorithms.
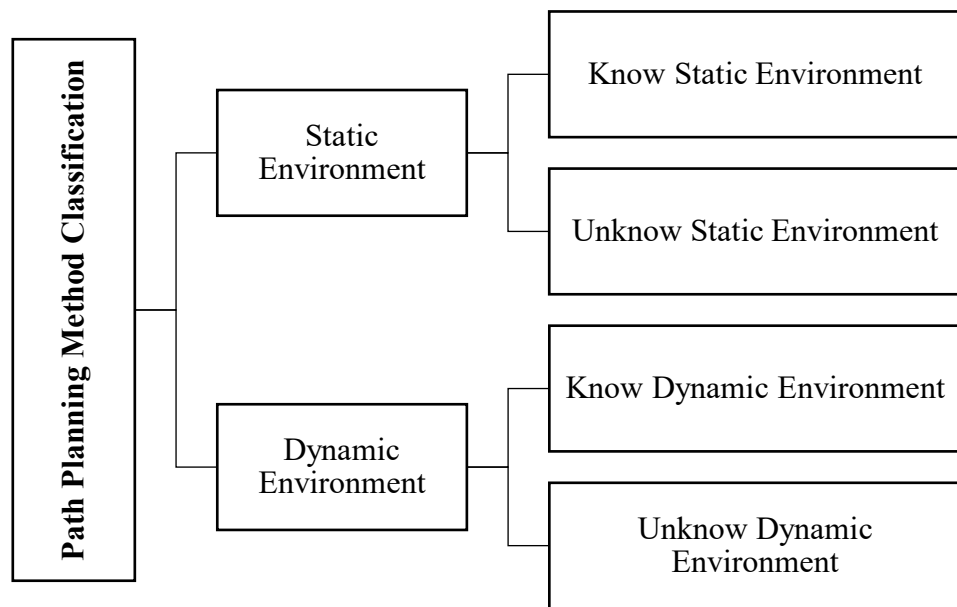
*Fig. 36 Robot Path Planning Classification*

Cao et al. in their publication, Region filling operations with random obstacle avoidance for mobile robots (1988), defines the criteria for the region filling operation (for a mobile robot) as follows:

1.  Robot must move through an entire area (cover the whole area)
2.  Robot must fill the region without overlapping path
3.  Continuous and sequential operation without any repetition of paths is required
4.  Robot must avoid all obstacles
5.  Simple motion trajectories (e.g. straight lines or circles) should be used (for simplicity in control)
6.  An "optimal" path is desired under available conditions.

Not always possible to satisfy all these criteria, particularly in agricultural fields, due to a shape not always regular and a presence of obstacles of different nature, priority consideration is required.

The problem of coverage path takes the idea from a variant of the of the traveling salesman problem (TSP), where to minimize the length of the travel,

each agent must visit not only each city but also the entire neighbourhood (Choset 2001, Arkin and Refael 1994).

As is well known, the TSP is an NP-hard problem in combinatorial optimization. NP-hard problems are problems for which there is no known polynomial algorithm, so that the time to find a solution grows exponentially with problem size. Arkin et al. (1993) have proved with the "lawnmower problem" that the problem of coverage path planning is NP-hard.

One approach typically used in global approaches is cellular decomposition. Cellular decomposition of the free space is used in many algorithms either implicitly or explicitly. This involves subdividing the region into sub-regions (typically trapezoids or triangles), find the best way to cover each sub-region, and then aggregate the results. The cellular decomposition algorithms can be classified into three classes: approximate, semi-approximate and exact (Latombe 1991, Choset 2001).

Exact cellular decomposition method to the agricultural environment was analysed by Oksanen and Visala (2007). The first approach was to first subdivide field using the standard plane-sweep algorithm to decompose the area into trapezoids. Then the sub-regions were merged into as large as possible areas. The merged region was then broken off and travelled in the same direction as the parallel sides of the trapezoids. The algorithm repeated on the remaining sub-areas until the entire field was covered. The "best" region was determined by a weighted sum of three factors: area, distance travelled, and turning times. This study particularly points out the costs of traveling in a particular direction.

Some floor-cleaning robots rely on the randomization approach. If you sweep the floor randomly long enough, it should become cleaned. The main advantages to this approach include the only needs of sensors to detect the hit to boundaries, no needs for localization sensors, thus no complex algorithms are needed onboard. Blach demonstrates that the efficiency of robots with random algorithms is approximately 20% with respect of ones that use more advanced methods. As a consequence, if a robot with a random algorithm can be constructed

at 1/5 of the price of one with localization and advanced path planning, it is cost-efficient (Balch 2000, Choset 2001). However, for agricultural field operations, it is difficult to think that random approach could be usable, as the cost of operating the vehicle, fuel and time, would be extremely expensive, and not in line with the principles of sustainability.

An online coverage algorithm, proposed by Gonzalez et al. (2005), uses spiral filling paths instead of back and forth paths. The algorithm subdivides the workspace into simple regions as the area is covered.

Others approach make use of artificial intelligence to solve the path planning problem in a static environment. Research exists in the area of genetic algorithms, neural networks, ant colony optimization algorithms, etc.

## 5.4.2.    Path Planning Approach

Agricultural machines are normally driven by human operators who design a driving strategy for themselves based on the type of task, on the type of machine to be used but above all on the experience acquired over the time.

Autonomous field machines will work the fields, sooner or later. The new issues for autonomous operation are safety, detection of failures, recovering after failures, and automatic refilling or emptying. If a human driver no longer operates the machine, automatic path planning is also needed; the robot has to find a route to execute the task. An optimal solution would be perfect, but a valid solution near optimal would be sufficient in most cases. (Oksanen T., 2007).

It is assumed, with respect to the environment, the field boundaries and eventually obstacles position are known. Here the environment is assumed to be fixed and the current position and attitude measured precisely.

In this chapter, an algorithm to solve the coverage path planning problem is presented. The approach adopted is based on the Boustrophedon Cell Decomposition (BCD). The boustrophedon cell decomposition approach is well

known, but here that is extended to support the special requirements of agricultural field machines and agricultural fields.

Boustrophedon is a Greek word and literally means "the way of the ox", is a task, originally writing, that proceeds in one direction in one line (such as from left to right) and then in the reverse direction in the next line (such as from right to left).

The boustrophedon cellular decomposition is a variant of a trapezoidal exact cellular decomposition approach, for the purpose of coverage area.

Cellular decomposition is a motion planning technique in which the free space (the robot does not overlap an obstacle) is decomposed into cells such that the union of the cells is the original free space. Each cell can be represented as a node in a graph. Cells are adjacent when share at least one edge. This graph is called an adjacency graph. If each cell can be covered by the robot, then the coverage problem reduces to determining a walk through the adjacency graph that visits each node at least once, i.e., TSP, for which a solution always exists. (H. Choset, P. Pignon, 1997). An example is shown in Fig. 37.
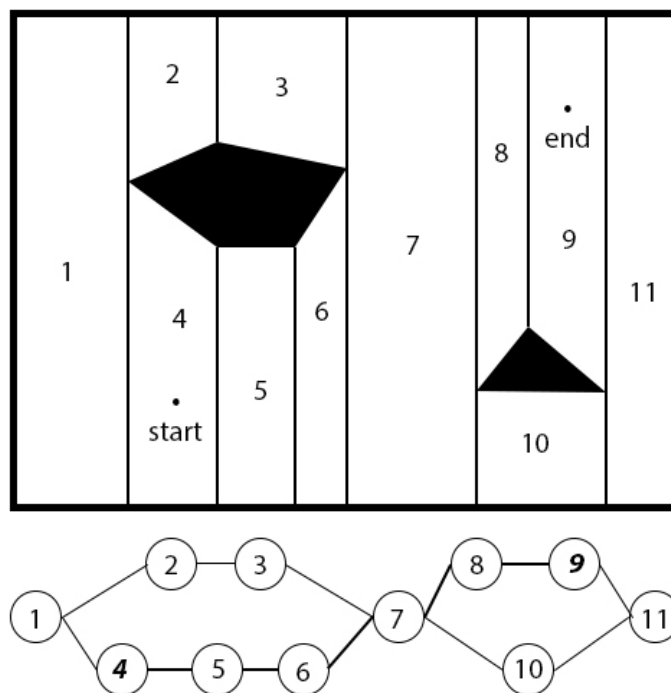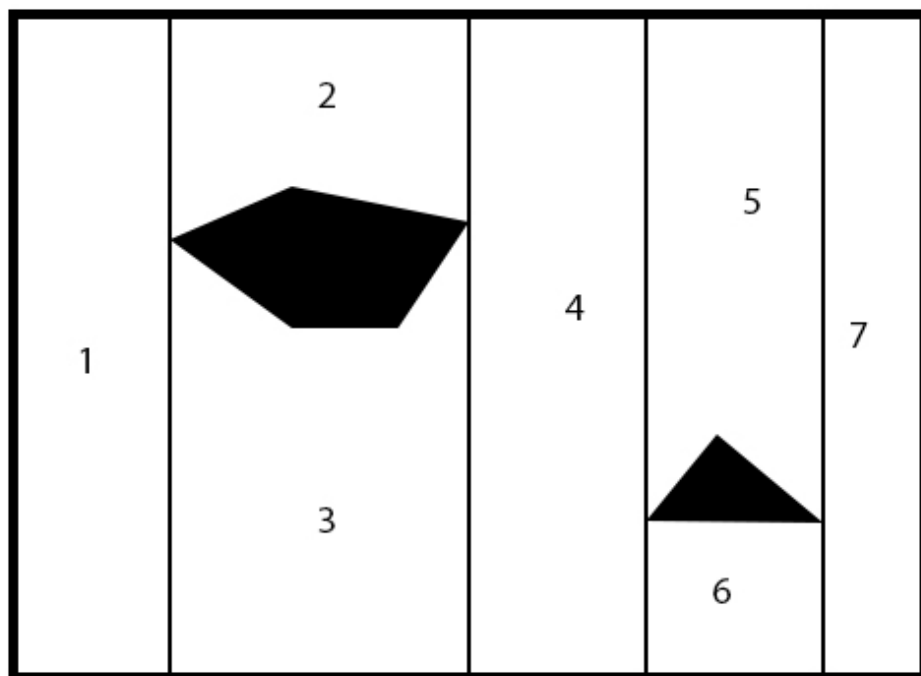


*Fig. 37 Exact Cellular Decomposition – Trapezoidal Decomposition*

The boustrophedon decomposition is designed to minimize the number of excess lengthwise motions, reducing the number of cells. It is formed by considering the vertices at which a vertical line can be extended both up and down in the free space. Straight line segments constructed at these vertices between the obstacle boundaries form the cell boundaries in the free space (Fig. 38).

Instead of treating all points as "events" where a subdivision is to occur (the idea in which the trapezoidal decomposition relies on), subdivision only occurs at "IN" events (split point) and "OUT" events (merge point). At an IN event, the current cell (if any) is closed and two cells are opened. At an out event, two cells are closed, and one cell is opened (assuming it's not the last point on the outer boundary). At all other points, the shape of the cell is simply updated. Each cell was then covered using back and forth paths. The choice of the sweep direction can affect the optimality of the solution.



*Fig. 38 Exact Cellular Decomposition – Boustrophedon Decomposition*

### 5.4.3.    Map Reference Coordinate System

It is possible, from the Pix4Dmapper, to export a georeferenced Application Map as a "geotiff" (.tif) or "shapefile" (.shp) to be imported in any Tractors Consoles.

A georeferenced Map is going to be used in order to plan the covering path algorithm.

The GeoTIFF map the "Pix4Dmapper" generates, presents an "EPSG:32720 - WGS 84 / UTM zone 20S" coordinate reference system (CRS)

EPSG stands for European Petroleum Survey Group. They publish a Geodetic Parameter Dataset of Coordinate Reference Systems and Coordinate Transformations. The numbers '32720' corresponds to the projection related to this project region (NIMA Technical Report 8350.2).

WGS 84 (World Geodetic System 1984) is an Earth-centered, Earth-fixed terrestrial reference system and geodetic datum. WGS 84 is based on a consistent set of constants and model parameters that describe the Earth's size, shape, and gravity and geomagnetic fields.

The Universal Transverse Mercator (UTM) conformal projection uses a 2-dimensional Cartesian coordinate system to give locations on the surface of the Earth. Like the traditional method of latitude and longitude, it is a horizontal position representation, i.e. it is used to identify locations on the Earth independently of vertical position. However, it differs from that method in several aspects. The UTM system is not a single map projection. The system instead divides the Earth into sixty zones, each being a six-degree band of longitude, and uses a secant transverse Mercator projection in each zone. The map projection of this project corresponds to 20S UTM zone.

The coordinates unit of measure of this CRS is in meters and in particular, according to the experimental field, each 7 pixels on X or Y-axis correspond to about 0.97 meters ($1mt = \frac{7}{0.97} = 7.2165\ pixels$).

In order to work with Latitude and Longitude coordinates we have to convert the UTM system to Decimal Degrees (DD) reference system.

According to World Geodetic System, the radius of the semi-major axis of the Earth at the equator is 6,378,137.0 meters resulting in a circumference of 40,075,161.2 meters. The equator is divided into 360 degrees of longitude, so each degree at the equator represents 111,319.9 meters or approximately 111.32 km. As one moves away from the equator towards a pole, however, one degree of longitude is multiplied by the cosine of the latitude, decreasing the distance, approaching zero at the pole. Knowing that the experimental field is located about the 33rd south parallel, the following table (Tab. 5) is derived.

To calculate these values, take the values in length at the equator and multiplicate them for the cosine of the latitude. These values are valid for what concern the longitude, it means for the values on X-axis.

| decimal degrees | DMS | N/S or E/W at equator | E/W at 33N/S |
|---|---|---|---|
| 1 | 1° 00′ 0″ | 111.32 km | 93.36 km |
| 0.1 | 0° 06′ 0″ | 11.132 km | 9.336 km |
| 0.01 | 0° 00′ 36″ | 1.1132 km | 933.6 m |
| 0.001 | 0° 00′ 3.6″ | 111.32 m | 93.36 m |
| 0.0001 | 0° 00′ 0.36″ | 11.132 m | 9.336 m |
| 0.00001 | 0° 00′ 0.036″ | 1.1132 m | 933.6 mm |
| 0.000001 | 0° 00′ 0.0036″ | 111.32 mm | 93.36 mm |

*Tab. 9 Degree precision versus length*

For the latitude values, Y-axis, as the parallels are equally spaced, the length values used are the relative ones at the equator.

Let's find the exact match between 1 meter and decimal degrees

- For X-axis: $\quad x : 1 = 0.00001 : 0.9336 \Rightarrow$

$$\Rightarrow x = \frac{0.00001}{0.9336} = 0.00001071122 \; decimal \; degrees$$

- For Y-axis: $\quad y : 1 = 0.00001 : 1.1132 \Rightarrow$

$$\Rightarrow y = \frac{0.00001}{1.1132} = 0.00000898311 \; decimal \; degrees$$

Now according to Decimal Degree Georeferenced Map, for the X-axis, each Pixel on the map correspond to a difference of about 0.0000014466 decimal degrees, it derives that:

$$x : 0.00001071122 = 1 : 0.0000012699 \Rightarrow$$

$$\Rightarrow x = \frac{0.00001071122}{0.0000014466} \cong 7.4044 \; pixels$$

Thus, on X-axis, rounding, $\mathbf{1 \; mt = \; 7.5 \; pixels}$.

The same reasoning can be applied to the Y-axis, where each pixel corresponds to a difference of about 0.0000012699 decimal degrees, same as X-axis, so:

$$y : 0.00000898311 = 1 : 0.0000012699 \Rightarrow$$

$$\Rightarrow y = \frac{0.00000898311}{0.0000012699} \cong 7,0739 \; pixels$$

So, on Y-axis, it is possible to round the equality to $\mathbf{1 \; mt = \; 7 \; pixels}$.

## 5.4.4.    Algorithm Code

First of all, the algorithm will be developed using Matlab. Particular attention should be placed in saying that in order to execute the code, it will be necessary to install four Toolboxes: 'Mapping Toolbox', 'Image Processing Toolbox' and 'Statistics and Machine Learning Toolbox', from MathWorks

library, and 'utm2deg' add-on. This last function is useful just in case you want to work with Decimal Degree coordinate reference system instead of UTM one.

### 5.4.4.1. Read and Show Georeferenced Map

As said in the paragraph 6.4.2, we are going to work with a georeferenced map (.tif) of the region of interest, which includes a coordinate reference system datums based on UTM classification.

Using the integrated 'Mapping Toolbox' integrated function, `geotiffread` and `mapshow`, it is able to read and show the field georeferenced map (Fig. 39).

*Matlab Code:*

```
% read geotif RGBA image with Universal Transverse Mercator(UTM)
% coordinate system
map = '2018-10-05_lote22_msp_rgba_gndvi.tif';
[geotif_UTM, spo_UTM] = geotiffread(map);
geotif = geotif_UTM(:,:,1:3); % remove the 4-th channel (opacity)
mapshow(geotif, spo_UTM)
```
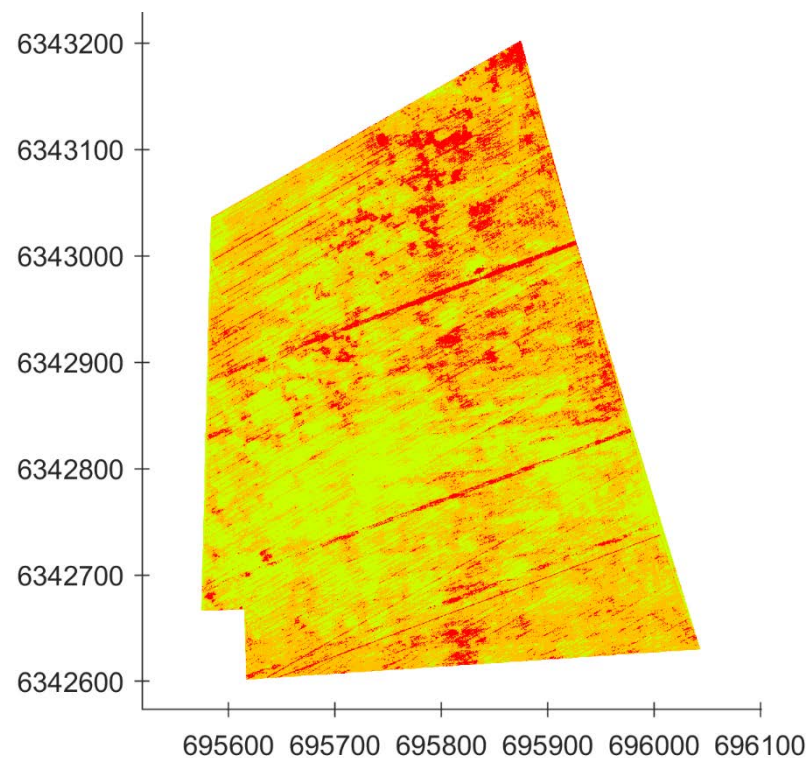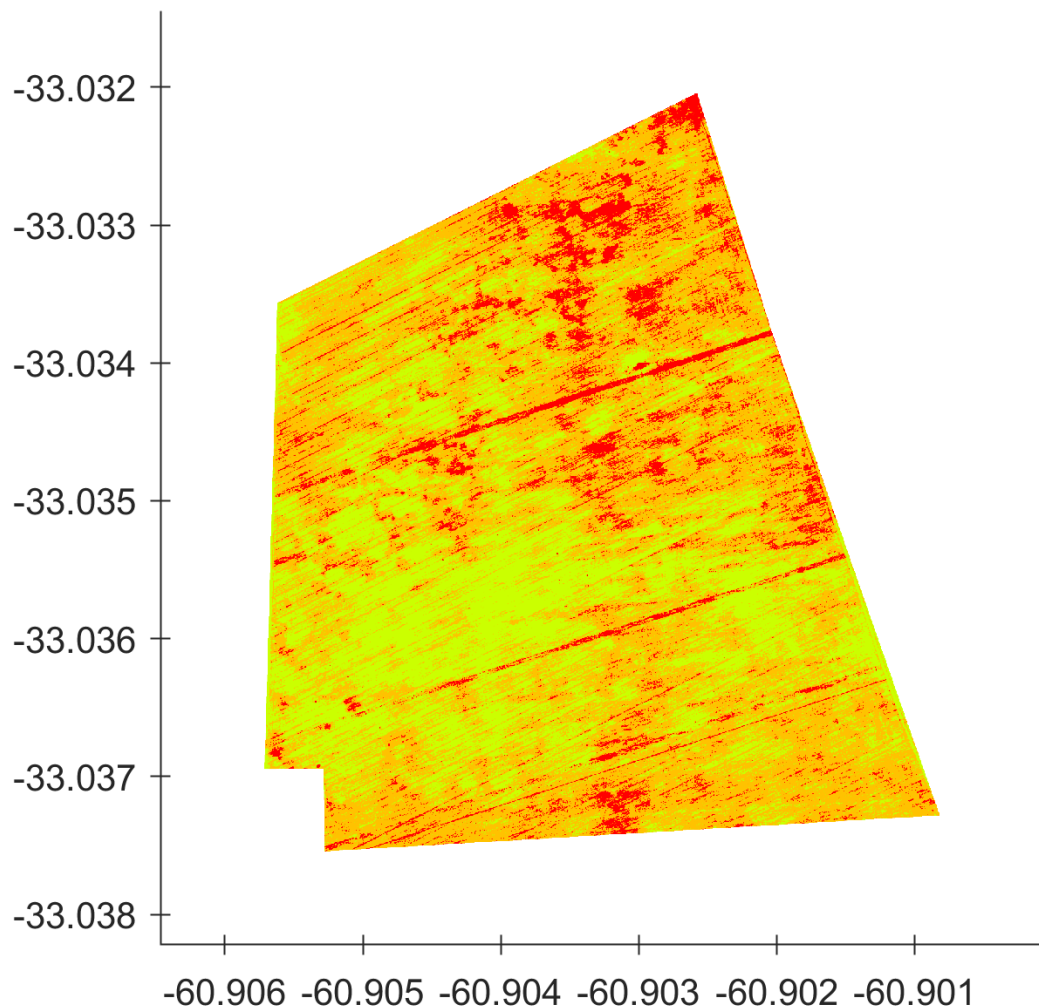


*Fig. 39 UTM Georeferenced Map*

Instead if need to work with decimal degree, convert it calling the function `utm2deg` obtaining the new map, Fig. 40.

*Matlab Code:*

```matlab
%% convert from UTM to Decimal Degree coordinates reference system
% input: original UTM crs, UTM zone (ex. '09 S')
% output: new Decinal Degree crs
function UTMref = utm2dd(UTMref, UTMzone)
utm_zone = UTMzone;
for i = 2:size(UTMref.XWorldLimits,2)
    UTMzone = [UTMzone; utm_zone];
end
[Lat, Lon] = utm2deg(UTMref.XWorldLimits', UTMref.YWorldLimits', ...
            UTMzone);
UTMref.XWorldLimits = Lon';
UTMref.YWorldLimits = Lat';
% UTMref.CellExtentInWorldX = UTMref.CellExtentInWorldY;
end
```



*Fig. 40 Decimal Degree Georeferenced Map*

## 5.4.4.2. Obstacle detection and Sub-Areas split

Two functions (`obstacle_row` and `obstacle_boundary`) are created to find possible obstacles within the lot.

For simplicity the RGB georeferenced map is converted to Black and White image (`im2bw` function) and all the path planning algorithm is based on it. Later the terms of "active area" or "active region" and "empty area" or "empty region" are going to be used to refer to, respectively, working area and non-working area of the field.

As can be seen from the previous pictures, the field on which we are experimenting does not contain any obstacle, so, only for study purpose, we create some of it.

The following line of code will explain how the obstacle detection and the field subdivision area functions work.

The `obstacle_row` function basically detect a change from an active area to an empty area, this mean that an obstacle has been found. This action is repeated for each map matrix row and each time a change is found. A variable (`no_obst`) stores the total number of obstacles contained in each row.

*Matlab code:*

```
%% save the position of and the number of obstacles in each row
% input: BW image(img), row position(i)
% output: n. of i-th row obstacles(no_obst) and its position(id_obst)
function [no_obst, id_obst] = obstacle_row(img,i)
id_obst = [];
no_obst = 1;
for j=2 : size(img,2)
    % if change from obstacle(0) to free space(1)
    if img(i,j-1)==0 && img(i,j)==1
        [right, left, ~, ~] = cells_check(img,i,j);
        % if cell has free spaces(1) on right and left is obstacle
        % otherwise it is boundary
        if left>1 && right>1
            no_obst = no_obst+1; % increase the n. of row obstacle
            id_obst = [id_obst; j-1]; % save obstacle column position
        end
    end
    % if change from free space(1) to obstacle(0)
    if img(i,j-1)==1 && img(i,j)==0
        [right, left, ~, ~] = cells_check(img,i,j);
```

```
        % if cell has free spaces(1) on right and left is obstacle
        % otherwise it is boundary
        if left>1 && right>1
            id_obst = [id_obst; j-1]; % save obstacle column position
        end
    end
end
end
```

Then the 'obstacle_boundary' function instead, reading the content of the 'no_obst' variable, when there is a change from a i-th row and the previous one, which is a change in the number of obstacles, is able to set the dividing line between one or more sub-region. Results in the definition of the total number of field area splitting.

*Matlab code:*

```
%% define upper and lower obstacle limits and number of sub-areas
% input: n. of obstacle for each row(no_obst), BW image(img)
% output: rows of starting and ending obstacle(obst_line),
%         n. of sub-areas(no_area)
function [obst_line, no_areas] = obstacle_boundary(no_obst, img)
obst_line = [];
no_areas = obstacle_row(img,1);
for i=2 : size(no_obst,1)
   % if n.obstacles of two adiacent rows is different
   if no_obst(i-1) ~= no_obst(i)
       % if n.obstacles of previous row is higher than actual row
       if no_obst(i-1) > no_obst(i)
          obst_line = [obst_line; i-1]; % save the previous row
position
          no_areas = no_areas+no_obst(i); % increase n.sub-areas by
actual row obstacles n.
       else % if n.obstacles  of actual row is higher than previous
row
          obst_line = [obst_line; i]; % save the actual row position
          no_areas = no_areas+no_obst(i); % increase n.sub-areas by
actual row obstacles n.
       end
   end
end
end
```

The following pictures (Fig. 41, Fig. 42 and Fig. 43) show the results obtained from the application of the above-mentioned function.
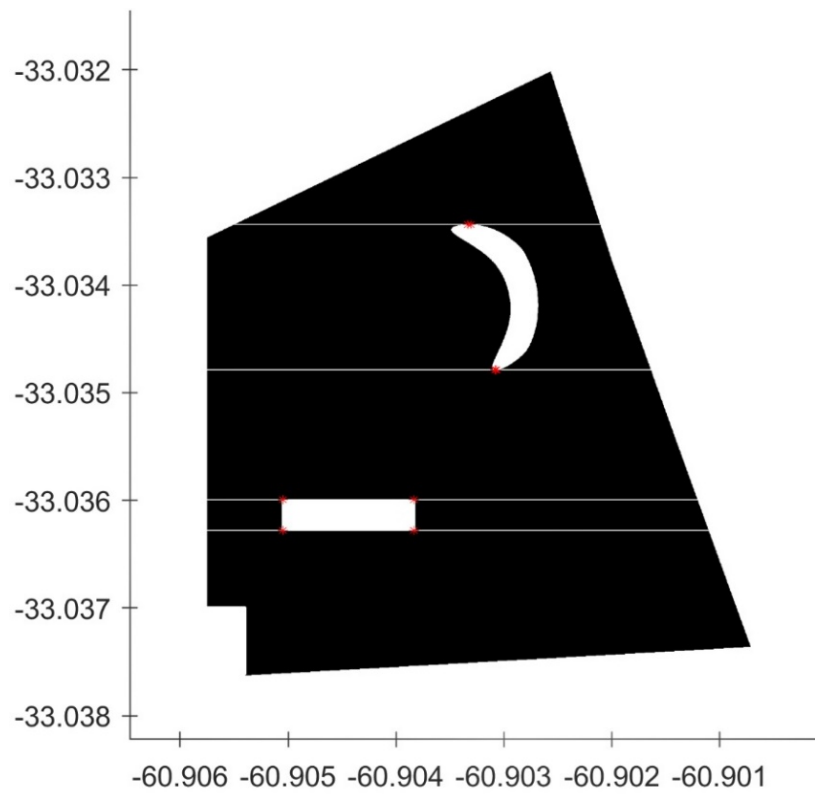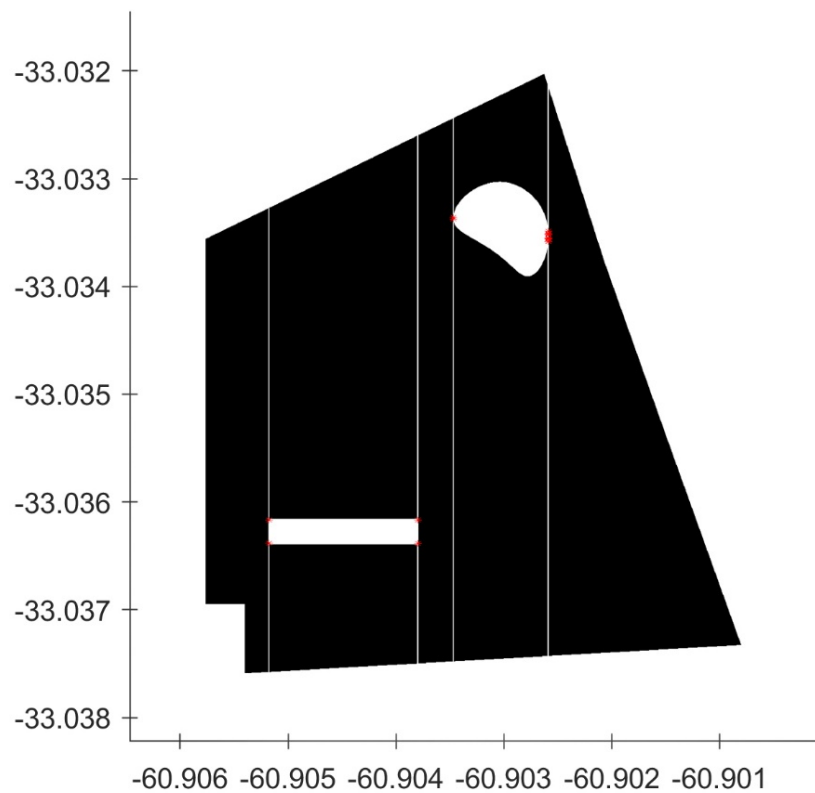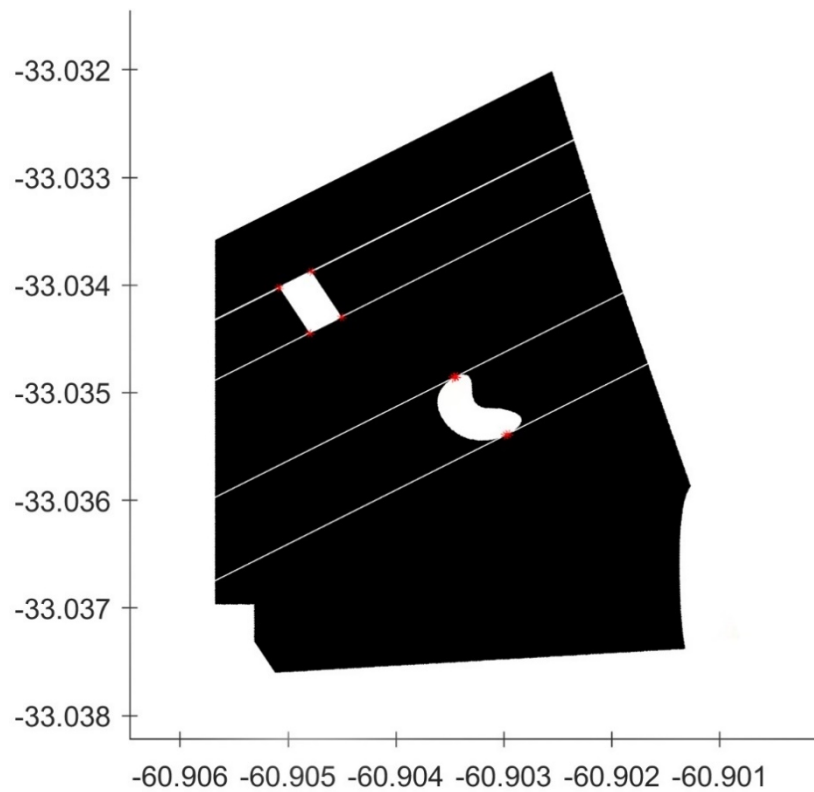
*Fig. 41 Field test 1 with obstacle*



*Fig. 42 Field test 2 with obstacle (90° rotated)*

*Fig. 43 Field test 3 with obstacle (30° rotated)*

It can be seen that, once an obstacle is found, the upper and lower limits are marked with a 'red star' points and empty lines (white) are drawn along these points. These lines divide the entire filed in sub-area. Then in each sub-region a working path is planned.

### 5.4.4.3. Path Creation Approach

To generate the working path another function, `create_path`, is invoked. The idea behind the code is simple. A cells variable of total sub-region number dimension, called `path`, is created. This variable contains all the planned tracks.

Essentially, after some checks, the path generation starts, moving from left to right of a row, to insert each pixel of a working area inside the `path` variable cell of the relative sub-area, until an obstacle is encountered, or the field boundary is reached.

When an obstacle is found, increase the cell index so the new path will be created in the next sub-area 'path' cell and so on until reaching the boundary point. If in the row there are no obstacles, the route creation will concern the same area.

Once the lot boundary is reached, a reverse procedure is used to the following row. Thus, moving from right to left, the path is crated until other side boundary is reached and every time and obstacle is found, the 'path' cell index is decreased, moving to the previous sub-region.

This procedure is repeated for every 'track row' of the map matrix. Track row mean the field virtual straight line (dashed blue line), see i.e. Fig. 45, which the tractor follows during the field manage operations. Therefore, this dashed blue line corresponds to the X-axis blue line passing on the tractor Centre of Gravity (Fig. 44).
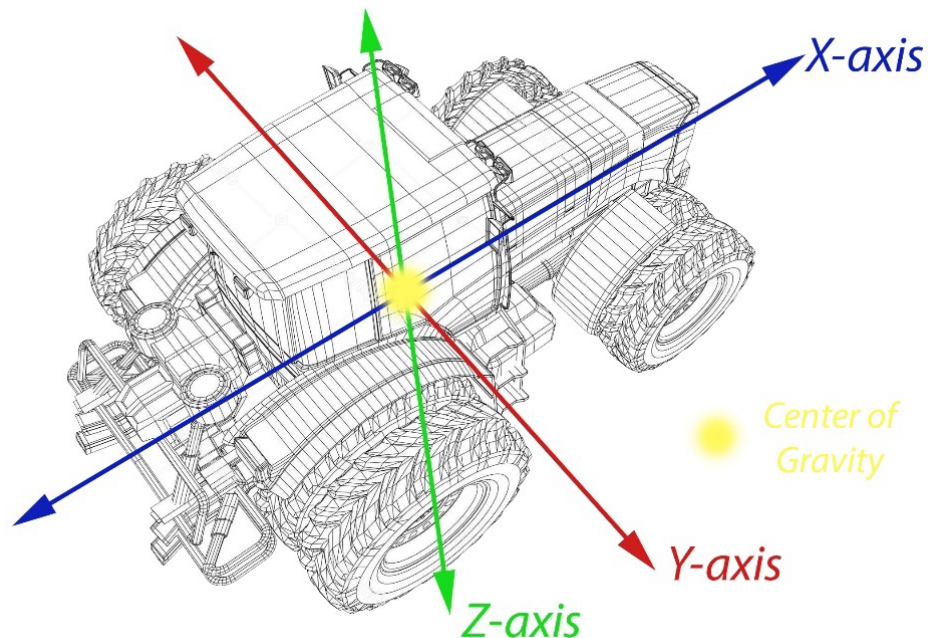


*Fig. 44 Tractor planes*

The track rows are equally spaced from each other of a certain distance (meters) according to the tool working width. For example, we suppose to use a towed fertilizer with a working width of 20 meters.

*Matlab code:*

```matlab
%% create working path
% input: BW image(img), n.obstacles(no_obst), obstacle limits
%     (obst_line), n.sub-areas(no_areas), tool working width(tool_width)
% output: working path, total covered distance(tot_actdist)
function [path, tot_actdist] = create_path(img, no_obst, obst_line,...
                                    no_areas, tool_width)
path = cell(no_areas,1);
active_dist = zeros(no_areas,1);
move = 0; % rightward move
k = 1;
obst_line = unique(obst_line);
temp = obst_line(1);
% creates a path each row with a step of dimension tool_width
for i=round(tool_width/2): tool_width: size(img,1)-round(tool_width/4)
    ...
    if img(i,:) == 0 % if row has all zero values skip to next one
        i = i+1;
    else
        if move == 0 % start rightward move
            for j=2 : size(img,2) % moving right on the row
                % if find an obstacle switch to next sub-path
                if img(i,j-1)==1 && img(i,j)==0
                    % if cell has free spaces(1) on right and left
                    % is obstacle otherwise it is boundary
                    [right, left, ~, ~] = cells_check(img, i, j);
                    if left>1 && right>1
                        k = k+1;
                    end
                end
                if img(i,j) == 0 % skip cell if it has zero value
                    continue;
                end
                % add cell to k-th path
                path{k} = [path{k}; j,i];
                % store the covered distance
                active_dist(k) = active_dist(k)+1;

            end
            move = 1; % row ends, next path moves leftward
        else
            if move == 1 % start lefttward move
                ...
                move = 0; % row ends, next path moves rightward
            end
        end
    end
end
tot_actdist = sum(active_dist); % total covered distance
end
```

The Fig. 45 picture show how the path generation code works on our experimental field while Fig. 46 is a detailed zoom-in of previous picture. Some test fields with obstacles are also analysed.
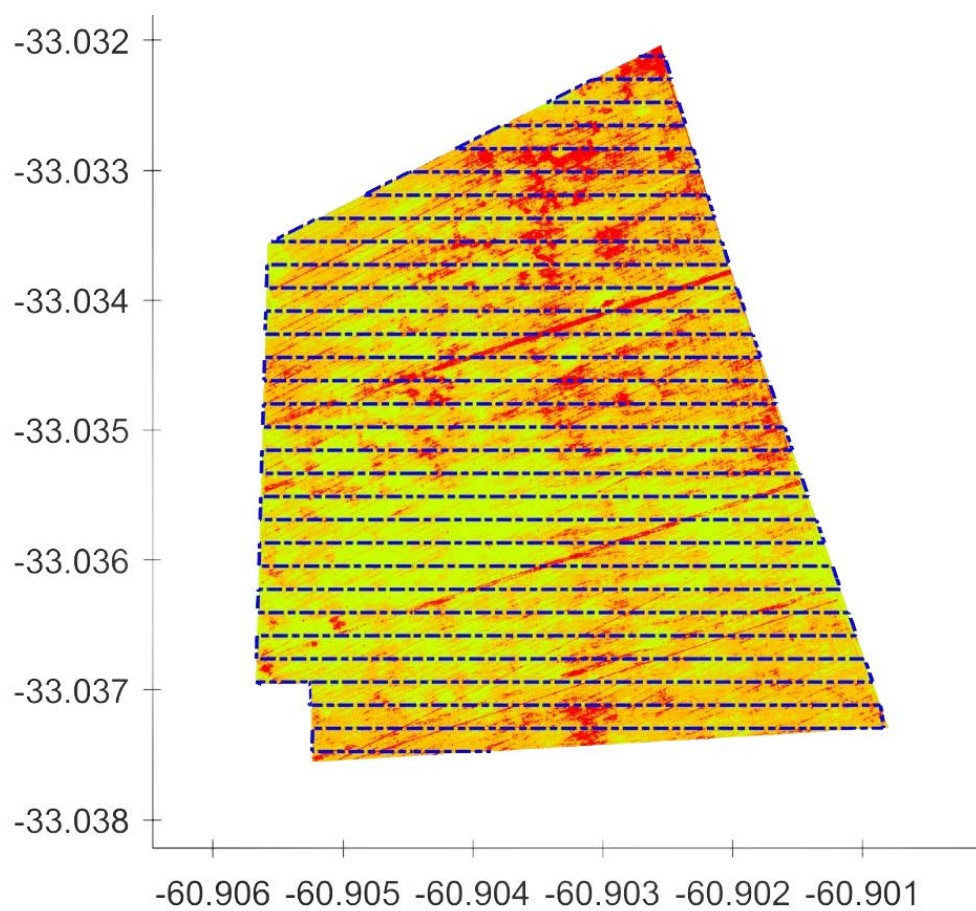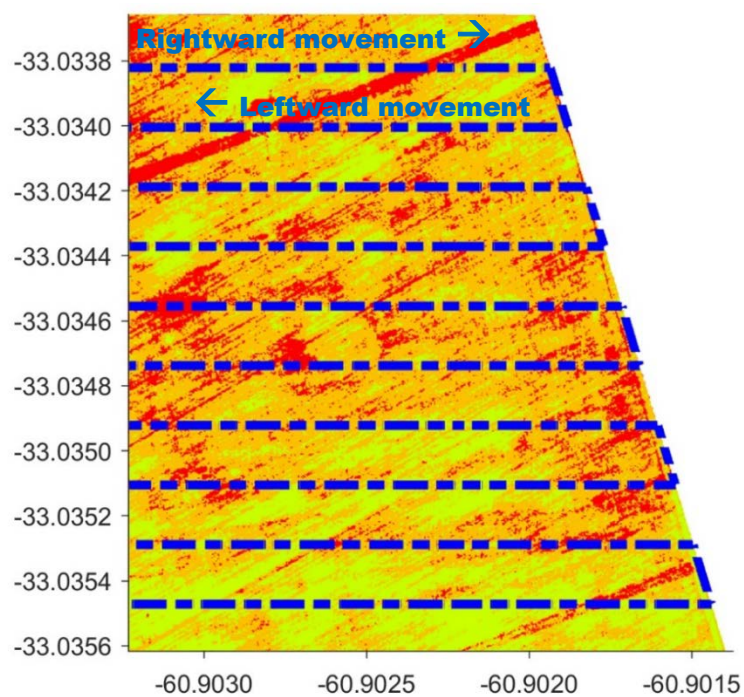
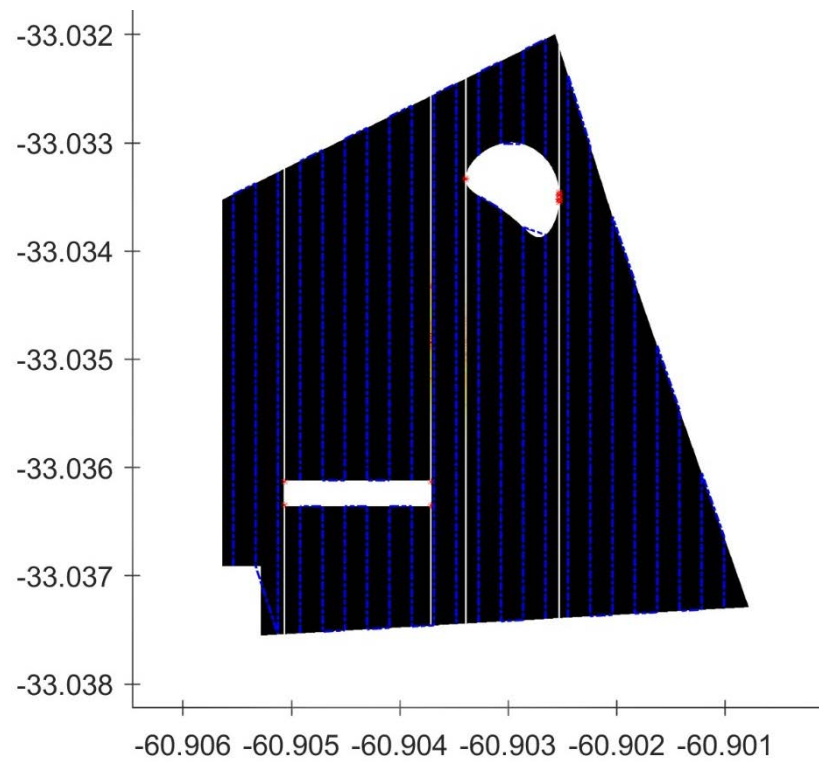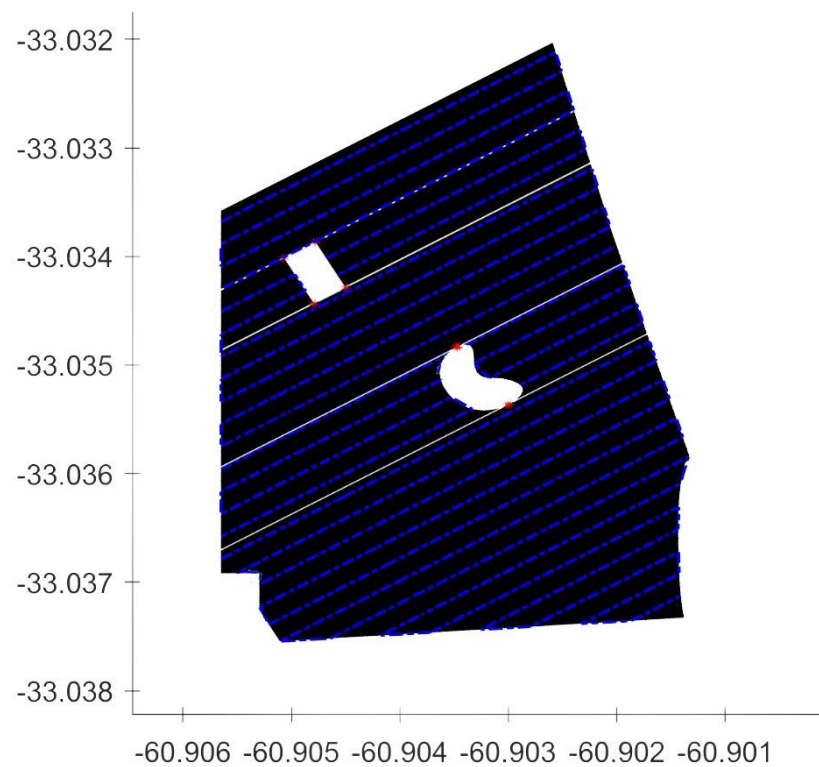*Fig. 45 Experimental Field Working Path*



*Fig. 46 Experimental Field Working Path detail*

*Fig. 47 Field test 2, with obstacles, Working Path*



*Fig. 48 Field 3, with obstacles, Working Path*

## 5.4.4.4. Headland Curve Creation Approach

The last step is to connect two adjacent working paths with an adequate curve of the agricultural machinery. Analysing the distance between each track, since it is wide enough, we opted for a C-type turn considering that it allows to minimize the space in the headland and consequently the time spent in performing it.

The code, wrote in the function 'headland_curve', basically generates one curve at the end of a trail and one at the beginning of a subsequent trail, and connect both with a straight line. The curve is generated from an exponential math operation based on the tractor curvature radius.

This math calculation changes a little when the intersection line between the last point of a track and the first point of the next track doesn't lie on the vertical plane (Y-axis), thus if it belongs to the 1st-3rd or 2nd-4th quadrants (Fig. 49, the arrows mean the machine movement direction). This is valid for both right-hand and left-hand turn.
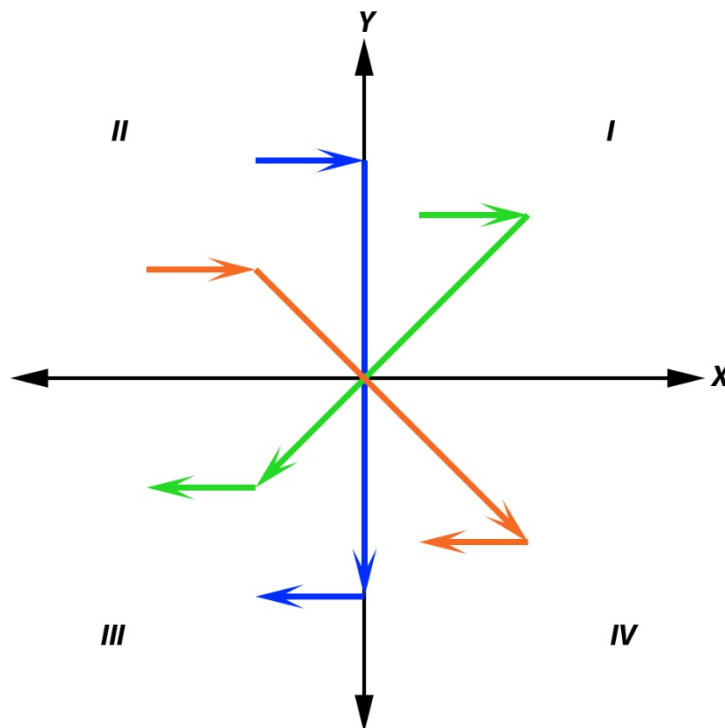


*Fig. 49 Quadrant Bisectors – Rightward Curve direction*

*Matlab code:*

```matlab
%% create a curve between each working path
% input: path, machine curvature radius(curvature_rad)
% output: new path including the curve path(path), total number of
%         curves(tot_curve), total curve distance(tot_inactdist)
function [path, tot_curve, tot_inactdist] = headland_curve(path, ...
                                           curvature_rad)
curvature_rad = curvature_rad*7;
newpts = 100;
num_curve = zeros(size(path)); % n. of headland curves in each path
inactive_dist = zeros(size(path)); % curve distance in each path
for l=1 : size(path)
    if isempty(path{l}) == 0 % skip empty path
        j = 1;
        cd = 0; %curve direction (0=right hand, 1=left hand)
        for m=2 : size(path{l,1})
            j = j+1;
            % moving from i-th working track to next one
            if path{l,1}(j-1,2) ~= path{l,1}(j,2)
                x = linspace(path{l}(j-1,1), path{l}(j,1), newpts);
                y = linspace(path{l}(j-1,2), path{l}(j,2), newpts);
                % create a line of points between end-point and
                 % next start-point
                pts = [x(:), y(:)];
                k = 1;
                ptx = []; pty = [];
                 % calculate distance between curve beginning and end
                inactive_dist(l)= inactive_dist(l)+curvature_rad*2+...
                    pdist([path{l}(j-1,:); path{l}(j,:)],'euclidean');
                if cd == 0 % generate right hand curve
                    % if bisector between starting and ending curve
                    % pts. lies on vertical axis
                    if path{l,1}(j-1,1) == path{l,1}(j,1)
                        % generate starting curve pts
                        for i=2 : round(newpts*0.1)
                            k = k+1;
                            ptx = [ptx; pts(i,1)+curvature_rad* ...
                                    exp(-1/k)];
                            pty = [pty; pts(i,2)];
                        end
                        % generate ending curve pts
                        for i=newpts-round(newpts*0.1)+1 : newpts-1
                            ptx = [ptx; pts(i,1)+curvature_rad* ...
                                    exp(-1/k)];
                            pty = [pty; pts(i,2)];
                            k = k-1;
                        end
                        pt = [ptx pty];
                        % insert curve into relative sub-path
                        path{l,1} = [path{l,1}(1:j-1,:); pt; ...
                                    path{l,1}(j:end,:)];
                        cd = 1; % set next curve to be left hand
                    else
                        % if bisector between starting and ending
                         % curve pts lies on 2nd-4th quadrant
                        if path{l,1}(j-1,1) < path{l,1}(j,1)
                            ...
```
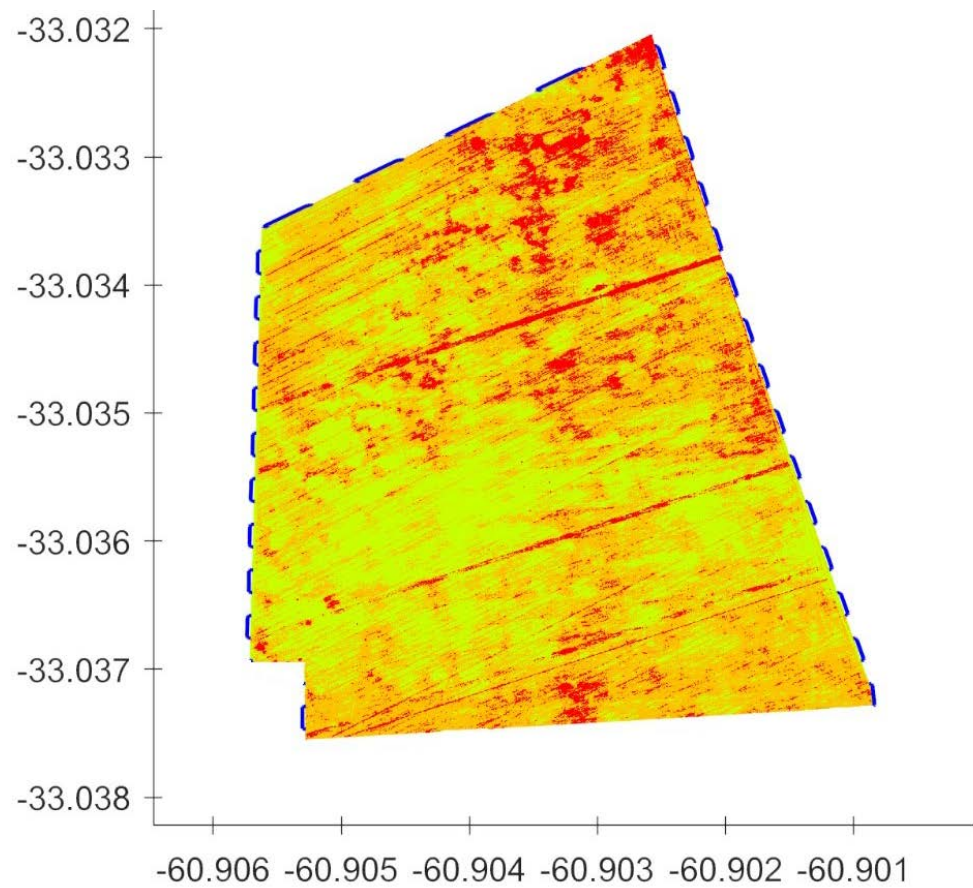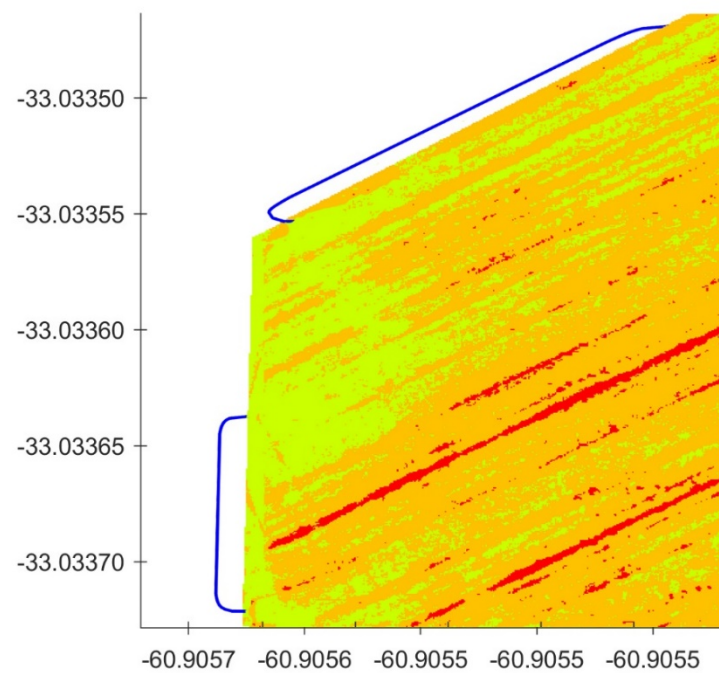
```matlab
                    else
                        % if bisector between starting and ending
                        % curve pts lies on 1st-3rd quadrant
                        if path{l,1}(j-1,1) > path{l,1}(j,1)
                            ...
                        end
                    end
                end
                num_curve(l) = num_curve(l)+1;
            else
                if cd == 1 % generate left hand curve
                    ...
                    num_curve(l) = num_curve(l)+1;
                end
            end
            j = j+size(pt,1);
        end
    end
    end
end
tot_curve = sum(num_curve); % total number of curves
tot_inactdist = sum(inactive_dist); % total covered distance
end
```

To demonstrate how the code behaves, few pictures are shown below. The field in question as well as some test fields are examined, and it is possible to see the subtle modifications between curves which presents different slope in the bisector line, as previously explained.

*Fig. 50 Experimental Field Headland Curves*



*Fig. 51 Experimental Field Headland Curves - Left Hand curve detail*
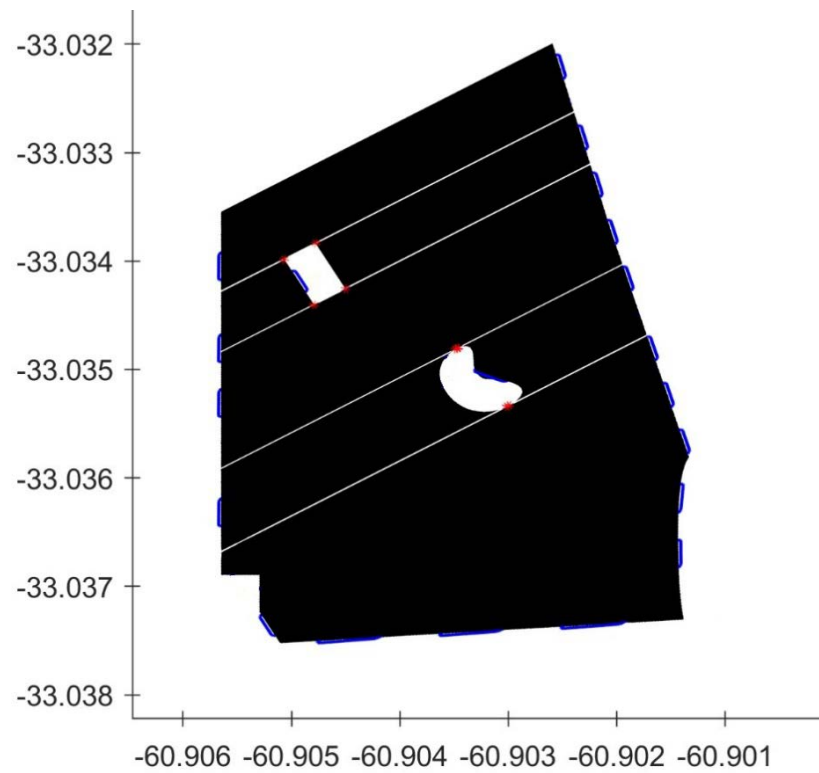
*Fig. 52 Field 3 Headland Curves*
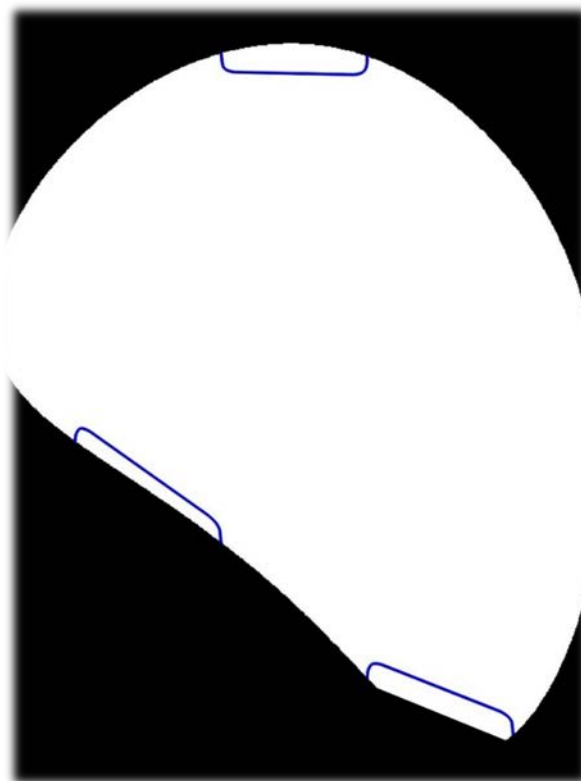


*Fig. 53 Field 2 Headland Curves detail*

### 5.4.4.5. Final Tests

In conclusion, each Matlab functions are merged together in order to provide a suitable dataset to be used for a real on-site planning.

For a deeper analysis, starts showing some pictures of our experimental field. The total field extension is about 20 ha.

Fig. 54 represents the original experimental lot in which the path follows the horizontal plane starting from top left corner until the lower right corner. While the next picture (Fig. 55) show different path rotated, from the original one, of a certain angle
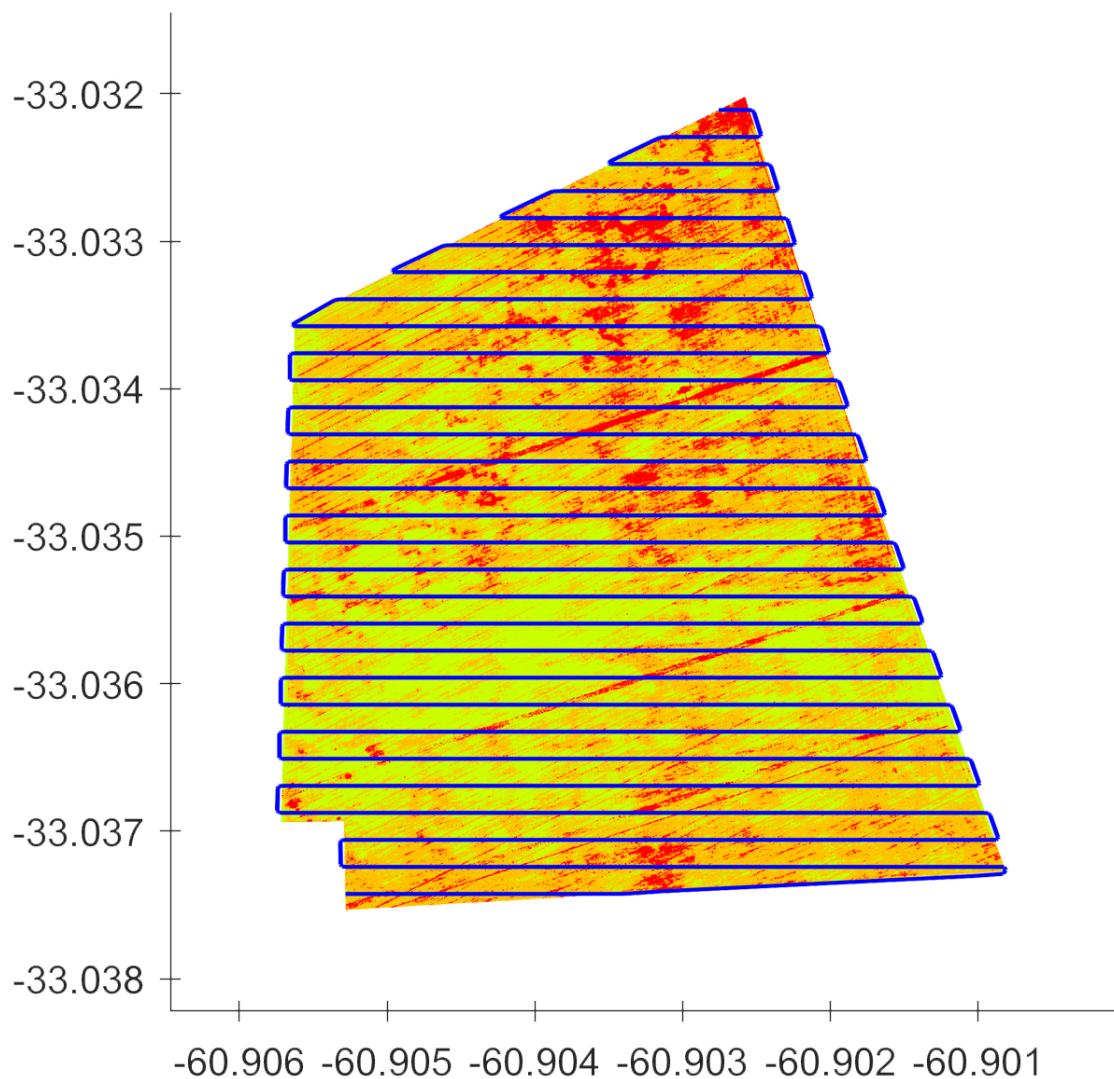


*Fig. 54 Experimental Field - Final Path Planning*

<table>
<tr><td>(a) 4° contraclockwise rotation</td><td>(b) 30° contraclockwise rotation</td></tr>
</table>

*(a) 4° contraclockwise rotation*

*(b) 30° contraclockwise rotation*

*(c) 88.5° contraclockwise rotation*

*(d) 106.5° contraclockwise rotation*
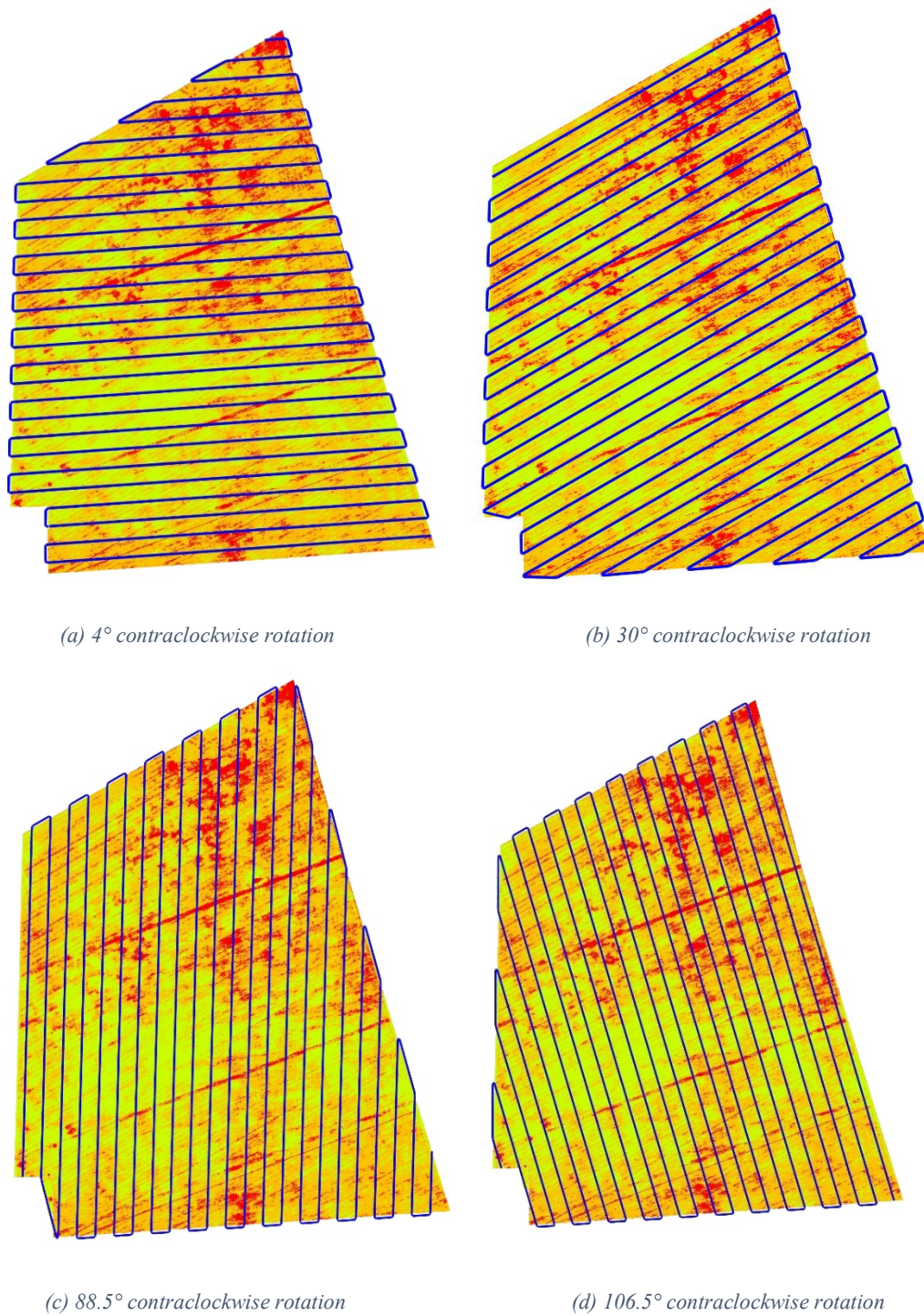
*Fig. 55 Experimental Field with different working path orientation*

The Matlab code execution returns in output some useful information. Particularly it is possible to know the total distance covered, including active tracks and curve path, and the total number of turns performed during the machine field operations. These data are listed in the table below (Tab. 10).

| Path Orientation (degree) | Total Distance Covered (meters) | Total Number of Curves |
|---|---|---|
| 0° | 10937 | 29 |
| 1.5° | **10526** | 28 |
| 4° | 10624 | 28 |
| 30° | 10752 | 28 |
| 88.5° | 10685 | 22 |
| 90° | 10730 | 22 |
| 106.5° | 10577 | **21** |

*Tab. 10 Experimental Field - Path analysis*

Analysing the information contained in this table is possible to notice how varying the path orientation, a change in terms of distance covered do not change in a significant way, this because, although modifying the path movement, the working area remains the same, while could change a lot the total number of curve in the path. The idea is to minimize both two values, prioritizing the number of curve, for the reason that they engrave on the total amount of inactive time spent.

In conclusion, between all the orientation angle examined, for what concern the total distance covered, the angle which present the minimum value belongs to 1.5° orientation angle; while, for the minimum number of curves in the path, we have to move until 106.5°.

Now focusing on which is the best path to choose, it is possible to study the improvement, or the worsening, in terms of distance covered and number of curves, comparing each path orientation angle data with the original path angle.

| Path Orientation (degree)\| | Tot Distance Covered improvement (%) | Tot Number of Curves improvement (%) | TOTAL (%) |
|---|---|---|---|
| 1.5° | **- 3.9** | - 3.6 | - 7.5 |
| 4° | - 2.9 | - 3.6 | - 6.5 |
| 30° | - 1.7 | - 3.6 | - 5.3 |
| 88.5° | - 2.4 | - 3.6 | - 6 |
| 90° | - 1.9 | - 31.8 | - 33.7 |
| 106.5° | - 3.4 | **- 38.1** | **- 41.5** |

*Tab. 11 Path Improvement Analysis*

Thus, the above table (Tab. 11) clearly shows that the best path is the one with an orientation angle of 106.5°, with the highest improvement of a total of 41.5 %, divided into a reduction of 3.4 % for the active working track and a reduction of 38.1 % for the curve path. The path is represented in the picture 'Fig. 55 (d)'.

For demonstrational purpose, the previous analysis is applied to the three parcel test containing obstacles (Fig. 56, Fig. 57 and Fig. 58) and the results are shown below (Tab. 12).
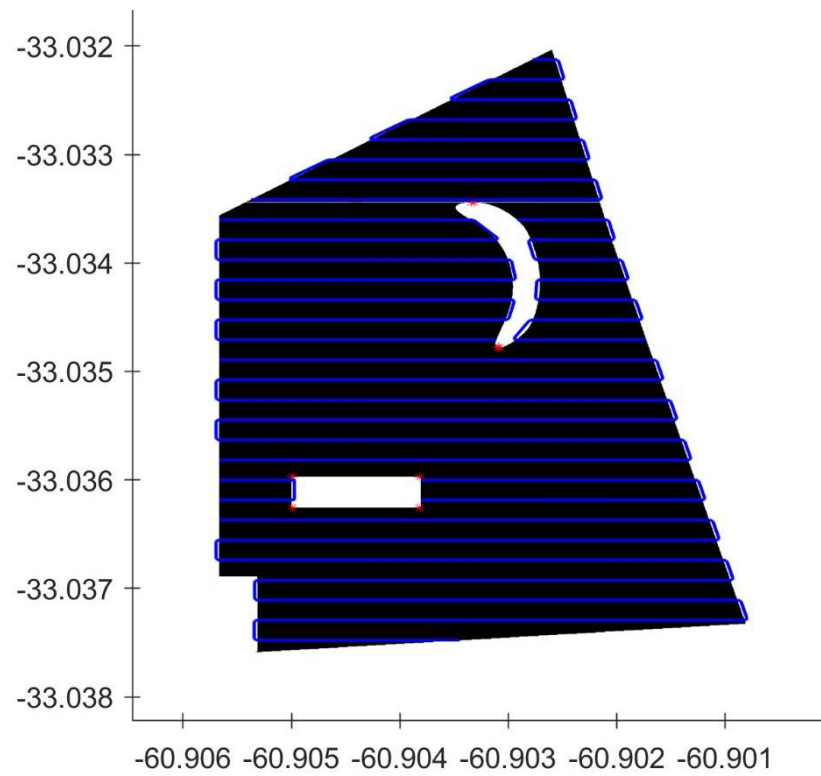
*Fig. 56 Field Test 1 - Final Path Planning (0°)*
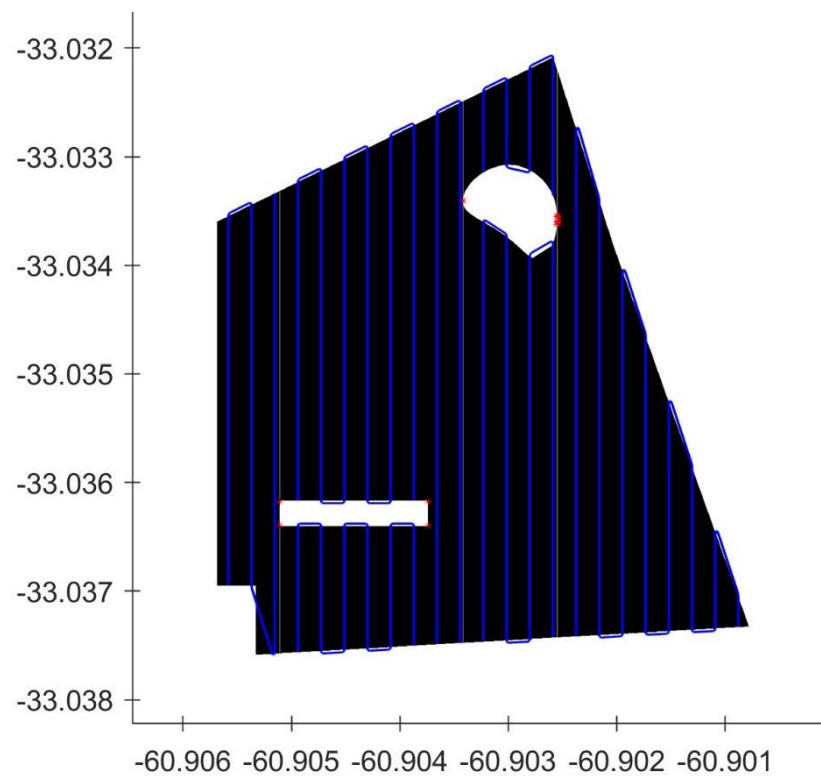


*Fig. 57 Field Test 2 - Final Path Planning (90°)*
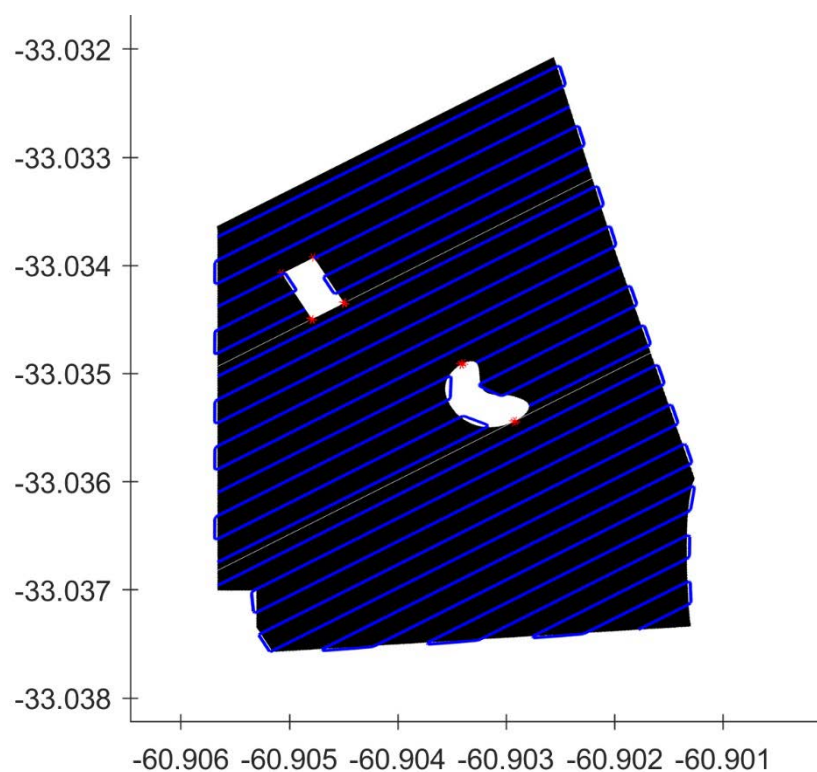
*Fig. 58 Field Test 3 - Final Path Planning (30°)*

| Field Test | Path Orientation (degree) | Total Distance Covered (meters) | Total Number of Curves | Total Improvement (%) |
|---|---|---|---|---|
| Field 1 | 0° | 10271 | 32 | - |
| Field 1 | 1.5° | 10065 | 31 | - 4.2 |
| Field 1 | 106.5° | 10091 | 24 | - 35 |
| Field 2 | 0° | 10335 | 30 | - |
| Field 2 | 1.5° | 10098 | 28 | - 9.4 |
| Field 2 | 90° | 10249 | 26 | - 16.1 |
| Field 3 | 0° | 10206 | 31 | - |
| Field 3 | 30° | 9876 | 27 | - 18.1 |
| Field 3 | 106.5° | 9954 | 18 | - 74.5 |

*Tab. 12 Field Test - Path Analysis*

As in the experimental field, also here the results can vary in a significant way changing the working path orientation.

Just for reference, some other picture with a different tool working width are shown below.
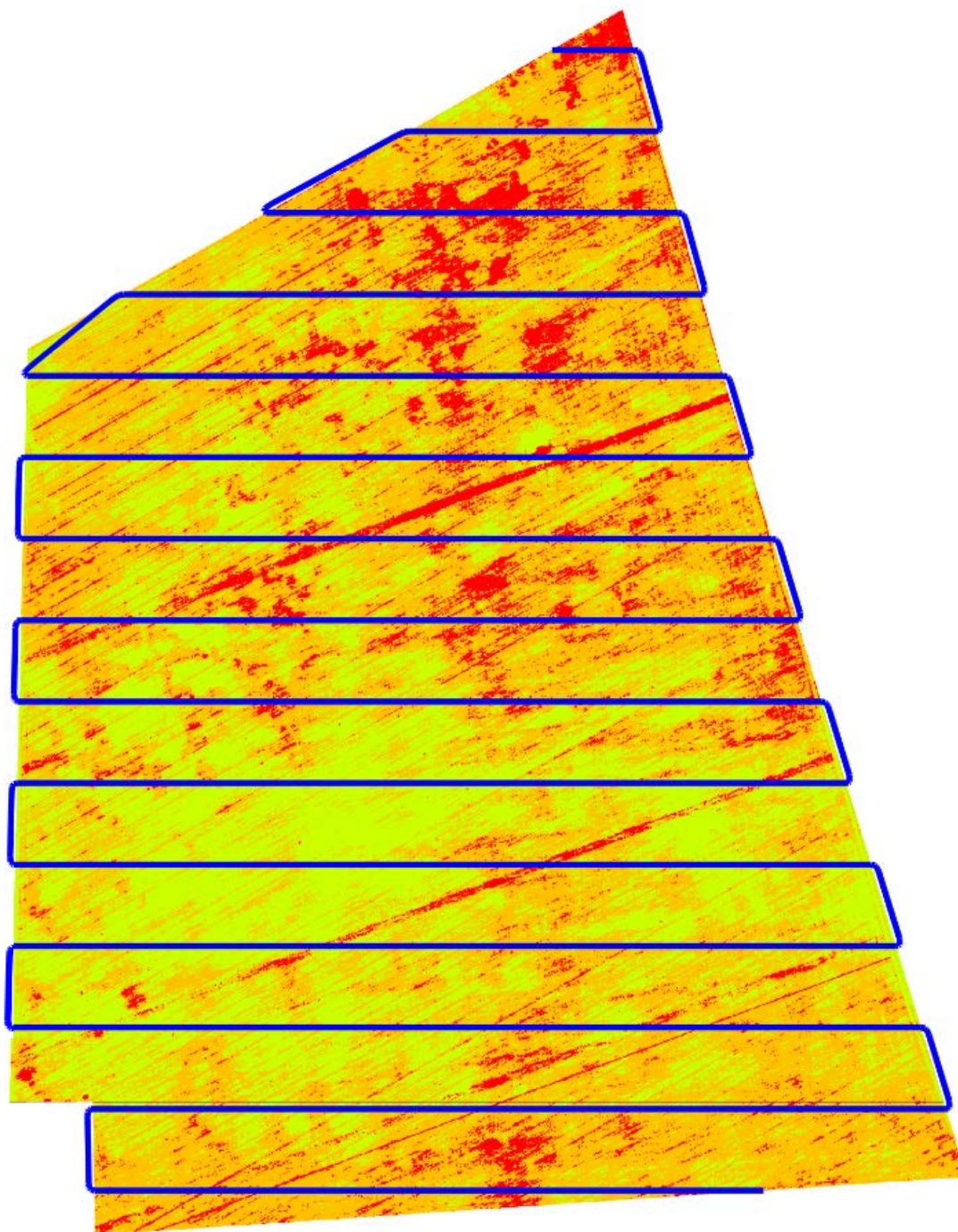


*Fig. 59 Experimental Field - 40 m tool's working width*

*Fig. 60 Experimental Field - 5 m tool's working width*

# 6. Conclusions and Future Developments

Coverage path planning is an important part of an intelligent agricultural field machine. The machine can be a traditional tractor driven by a human with a navigation system or an autonomous vehicle, a mobile robot.
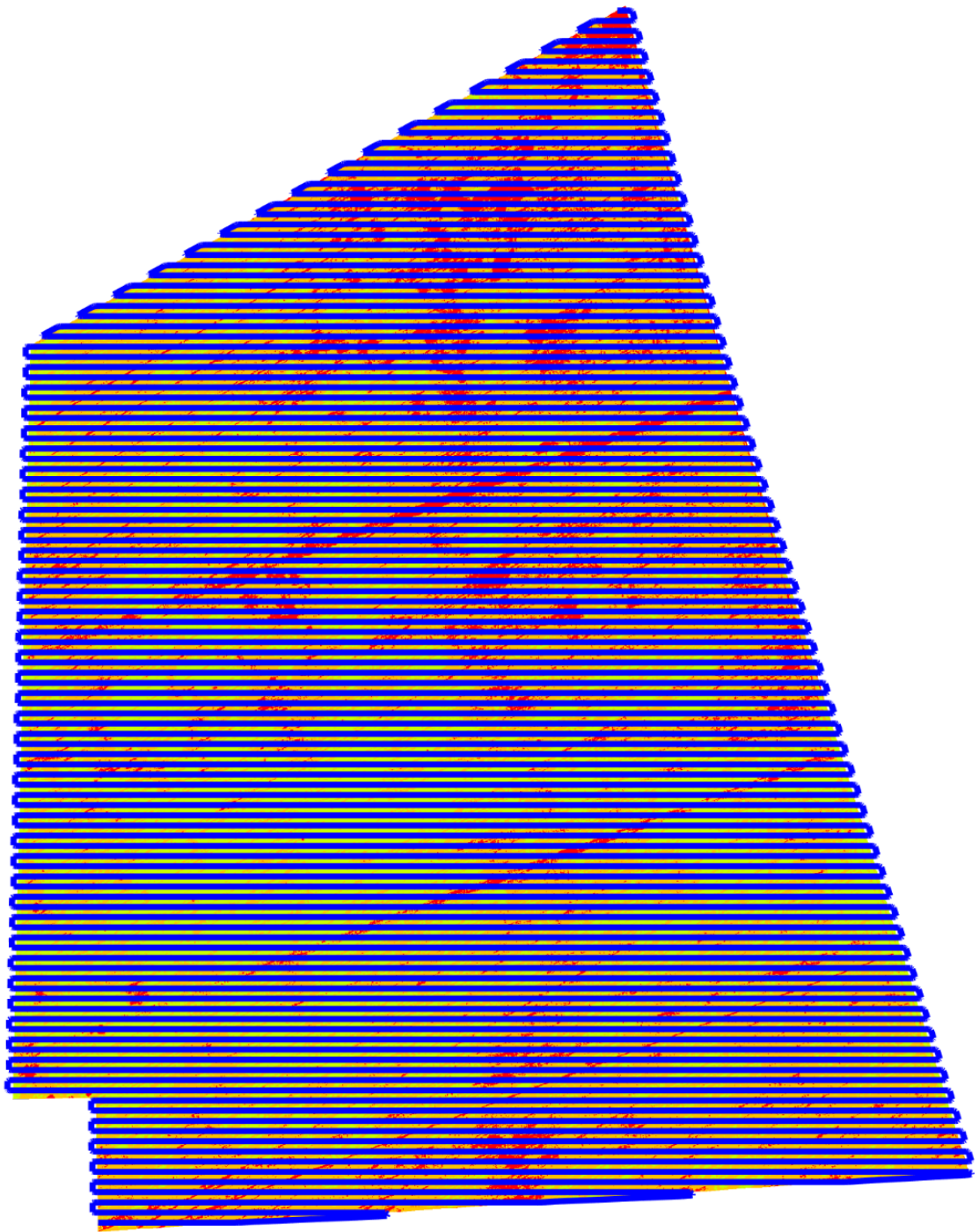
Considering all the previous studies, the research in the field of cellular decomposition seems one of the best approaches to lead to an optimal solution in the agricultural panorama. As the field boundaries and obstacle locations are generally well known in advance, there is no needs of an on-line implementation. The goal of this research was to analyse the crop heath status and field characteristics by RPAS multispectral photos and to create an algorithm that finds a reasonably efficient solution to the problem of completely covering a given field such that every point in the generated path is passed over by the machine.

The algorithm is based on a type of exact cellular decomposition approach termed the boustrophedon cellular decomposition. A robot can easily plan a boustrophedon motion in each cell of the boustrophedon decomposition. Once each cell is covered, the entire environment is covered. This approach sometimes skips portions of the environment near the boundaries of field and obstacles because of the discretization of the side step. If the robot has a shorter side step, these uncovered areas are reduced.

None of the algorithm analysed will solve the universal problem optimally being the problem NP-hard.

The algorithm presented in this thesis has been shown to be an efficient algorithm for finding a good solution for covering the field.

The process requires relatively low computational times than other algorithms proposed for solving the complete coverage path planning problem in an agricultural environment. The algorithm proposed here runs in O(n2) time while prior algorithms took as long as O(n3 log (n)) time.

All tests were run on a laptop with a 1.60 GHz Intel Core$^{TM}$ i5-8250U Quad-Core CPU, with 8 GB of RAM. A solution was found for all fields tested, including those with several interior boundaries, in less than 15 seconds, in case the tool working width is set to 20 meters, which increments the execution time in an exponential way if this width is reduced and, vice versa, reduce the time if it is increased.

There are some limitations, however, with this algorithm and several variations can be made to this algorithm to improve the optimality.

One optimization is to find the best orientation path running one test for each angle degree, but this will increase the running time to O (n3).

Regarding research area, this algorithm only operates in two dimensions. It does not take into account the effect of hills in planning the route. If the hills are particularly steep, then it would not be practical to travel in certain directions due to the slope. Finally, this algorithm does not consider the determination of optimal moment to stop and refuel, nor solve the problem of coordinating the work of several machines in the field.

Such implementation would be useful for tilling operation as harvesting, fertilization or weeding. In this scenario, the tractor with a towed fertilizer during the tillage operation gets empty and needs to be refilled. Finding the most optimal path that allows for efficient vehicle replenishment would also be useful but is not accounted for here.

Other interesting avenue as future work is strictly connected to the use of the multispectral map showed on the Chapter 4. Analysing such maps a matrix data containing all the sub-pixel information about the VI index is obtained. Therefore, an algorithm can be developed to automatically adequate the needs according to the health status of crop vegetation.

As example, suppose to perform a fertilization operation and the tractor tows a tool that has a working width of 20 meters, ten meters from one tractor side and the same from the other side. Nowadays, this kind of tools have the capability

to distribute the quantity of fertilizer in a smart way, can discretize the amount between each side or even better for each distribution nozzle . Thus, the idea is that while the tractor proceeds along the path, generated by the coverage path algorithm, analyse the map, for instance each ten meters, to get an average of vegetation health status on the region below the fertilizer tool and then determine the quantity of fertilizer to supply. Continue until the whole field is covered.

An additional future application could be to implement some sensor on-board the agricultural machine able to detect unwanted objects along the way and eventually readapt the path. This feature is really important in the scenario of security since it can prevent from unpleasant situations due to the presence of persons or animal and even the presence of other elements such as trees or debris brought from natural phenomenon (storms, earthquakes, floods, avalanche, etc.).

# 7. Bibliography

[1]   Auernhammer, H. 2001. "Precision farming - the environmental challenge". Computers and Electronics in Agriculture, Nº 30, p. 31-43.

[2]   Basso, B.; Ritchie, J.; Pierce, F.; Bragad, R.; Jones, J. 2001. "Spatial validation of crop models for precision agriculture" Agricultural Systems, Vol. 68, Nº 2. p. 97-112.

[3]   Brase, T. 2006. "Precision Agriculture". Thomson Delmar learning. New York: Clifton Park. 224 p.

[4]   Bullock D.S.; Bullock, D.G. 2000. "From agronomic research to farm management guidelines: A primer on the economics or information and precision technology". Precision Agriculture, Vol. 2, Nº 1, p. 71-101.

[5]   Chen, H.; Lan, Y.; Hoffmann, W.; Wu, W.; Zhang, S. 2008. "Development of a Data Acquisition and Processing System for Precision Agriculture". Agricultural Engineering International: the CIGR Ejournal. Manuscript. IT 08 001. Vol. 10.

[6]   Cox, G.; Harris, H.; Cox, D. 1999. Application of precision agriculture to sugar cane. En: Proceedings of the 4th International Conference on Precision Agriculture, St. Paul, MN, ed., P.C. Robert, R.H. Rust, and W.E. Larson, Madison, WI: American Society of Agronomy, Crop Science Society of America, and Soil Science Society of America, p. 753-766.

[7]   Cox, S. 2002. "Information technology: the global key to precision agriculture and sustainability". Computers and Electronics in Agriculture, Nº 36, p. 93-111.

[8]   Dampney, P.; Moore, M. 1998. Precision agriculture in England: Current practice and research-based advice to farmers. En: 4th International Conference on Precision Agriculture, July 19-22, 1998. St. Paul. MN (EUA). P. 661-674.

[9]   Gil, E. 2004. "El laboreo de precisión enfocado a la reducción de costes de cultivo". Vida rural, Vol. 193, p. 32-34.

[10]  Grenón, D. 1994. Agromática: Aplicaciones informáticas en la empresa agropecuaria. PNATTI. Subsecretaría de Informática y Desarrollo, SECyT, Buenos Aires, 155 pp.

[11] Hatfield, J. 2000. Precision Agriculture and Environmental Quality: Challenges for Research and Education. National Soil Tilth Laboratory, Agricultural Research Service, USDA, Ames, IA (USA).

[12] Kemerer, A.C. 2003. Utilización de imágenes satelitales en agricultura de precisión para delimitar zonas de manejo uniforme. Tesis de grado. Facultad de Agronomía, UNER. Oro Verde. Argentina

[13] Kravchenko, A.; Thelen, K.; Bullock, D.; Millar, N. 2005. "Management, topographical, and weather effects on spatial variability of crop grain yields". Agronomy Journal, Vol.97, p.514–523, 2005.

[14] Leon, C.; Shaw, D.; Cox, M.; Abshire, M.; Ward, B.; Wardlaw III, M.; Watson, C. 2003. "Utility of remote sensing in predicting crop and soil characteristics". Precision Agriculture, Nº 4, p. 359-384.

[15] Lowenberg-DeBoer, J.; Swinton, S. 1997. "Economics of site-specific management in agricultural crops". En Site-specific management for agricultural systems. ASA/CSSA/SSSA, Madison, WI. p. 369-396.

[16] Luchiari, A Jr.; Shanahan, J.; Francis, D.; Schlemmer, M.; Schepers, J.; Liebig, M., et al., 2000. "Strategies for establishing management zones for site specific nutrient management". En: Proc. 5th International Conference on Precision Agriculture. Precision Agriculture Center, ASA, CSSA and SSSA, MN (EUA)

[17] Maroni, J.; et al. "Mapeo de Rendimientos - Precisión para detectar variables inducidas en el cultivo". VI Congreso Argentino de Ingeniería Rural, CADIR 2000 y Avances en Ingeniería Agrícola 1998/2000. Editorial FAUBA. Argentina

[18] Melchiori, R. 2007. Agricultura de precisión en Entre Ríos, aspectos relacionados con la sustentabilidad. En: Caviglia, O.P; Paparotti, O.F.; Sasal, M.C. (Eds) Agricultura sustentable en Entre Ríos. p. 195-200.

[19] Moges, M.; Raun, W.; Mullen, R.; Freeman K.; Johnson G.; Solie J. 2004. "Evaluation of Green, Red, and Near Infrared Bands for Predicting Winter Wheat Biomass, Nitrogen Uptake, and Final Grain Yielg". Journal of Plant Nutrition, Vol. 27, Nº 8, p. 1431-1441.

[20] Moguillansky, G. 2005. "La importancia de la tecnología de la información y la comunicación para las industrias de recursos naturales". CEPAL - SERIE Desarrollo productivo Nº 164. Santiago, Chile.

[21] Pierce, F.J.; Anderson, N.; Colvin, T.; Schueller, J.; Humburg, D.; McLauglin, N. 1997. "Yield mapping". En F.J. Pierce et al. (ed.) The state of site-specific management for agriculture, ASA, CSSA, and SSSA, Madison, WI. p. 211–244.

[22] Pierce, FJ & P Nowak. 1999. "Aspects of precision agricultura". En: Spark, D. (ed) Advance in Agronomy Academic Press 67, p. 1-85.

[23] Roberts, D.; Green, R.; Adams, J. 1997. "Temporal and spatial patterns in vegetation and atmospheric properties from AVIRIS," Remote Sensing of the Environment, Vol. 62, Nº 3, pp. 223–240.

[24] Rouse, J.; Haas, R.; Schell, J.; Deering, D.; Harlan, J. 1974."Monitoring the vernal advancement and retrogradation (Green wave effect) of natural vegetation". NASA/GSFCT, Greenbelt, MD. USA.

[25] Sørensen, C.; Bochtis, D. 2009. "Information Systems and Management for Future Farming". International Commission of Agricultural and Biological Engineers, Section V. Conference, Technology and Management to Increase the Efficiency in Sustainable Agricultural Systems. Rosario, Argentina.

[26] Tilman, D.; Cassman, K.; Matson, P.; Naylor, R.; Polasky, S. 2002. "Agricultural sustainability and intensive production practices". Nature. Vol. 418, p. 671-677.

[27] Verhagen J.; Bouma J. 1997. "Modelling soil variability". En Pierce F.J., Sadler E.J. (ed), The state of site specific management for agriculture, ASA Publ., ASA, CSSA e SSSA, Madison, WI, USA. P. 55-68.

[28] Zhang, M.; Hendley, P.; Drost, D.; O'Neill, M.; Ustin, S. 1998. Corn and Soybean Yield Indicators Using Remotely Sensed Vegetation Index. In: Proc. 4th International Conference on Precision Agriculture. St. Paul. MN. USA.

[29] Zubillaga, M.; Carmona, M.; Latorre, A.; Falcon, M.; Barros, M. 2006. Estructura espacial de variables edáficas a nivel de lote en Vedia-Provincia de Buenos Aires. Actas del XX Congreso Argentino de la Ciencia del Suelo. Salta (Argentina). p.288.

[30] Rouse, J., R. Haas, J. Schell, and D. Deering. Monitoring Vegetation Systems in the Great Plains with ERTS. Third ERTS Symposium, NASA (1973): 309-317

[31] Gitelson, A., and M. Merzlyak. "Remote Sensing of Chlorophyll Concentration in Higher Plant Leaves." Advances in Space Research 22 (1998): 689-692

[32] Jenks, George F. 1967. "The Data Model Concept in Statistical Mapping", International Yearbook of Cartography 7: 186–190

[33] McMaster, Robert, "In Memoriam: George F. Jenks (1916–1996)". Cartography and Geographic Information Science. 24(1) p.56-59

[34] Timo Oksanen. Phat Planning Algorithm for Agriculture Field Machines (2007).

[35] Xiong-Zhe Han, Hak-Jin Kim, Hee-Chang Moon, Hoon-Je Woo, Jung-Hun Kim, Young-Joo Kim. Development of a Path Generation and Tracking Algorithm for a Korean Auto-guidance Tillage Tractor (2013)

[36] Murphy, R.R. 2000. Introduction to AI Robotics: p.316

[37] Cao, Z.L, Huang, Y. and Hall, E.L. 1988. Region filling operations with random obstacle avoidance for mobile robotics. Journal of Robotic Systems, Vol. 5(2):87-102.

[38] Choset, H. 2001. Coverage for robotics - A survey of recent results. Annals of Mathematics and Artificial Intelligence. Vol. 31:113-126.

[39] Arkin E.M. and Refael H. 1994. Approximation algorithms for the geometric covering salesman problem, Discrete Applied Mathematics. Vol. 55(3):197-218.

[40] Choset, H. 2001. Coverage for robotics - A survey of recent results. Annals of Mathematics and Artificial Intelligence. Vol. 31:113-126.

[41] Latombe, J.C., Barraquand J. 1991. Robot Motion Planning: A Distributed Representation Approach.

[42] University of Missouri. Notes on the SPT. (2004)

[43] Bondaz C., Garbarino I., Lázzari J. 2012. Relevamiento planialtimetrico para el estudio de erosion de un sector de la cuenca de la laguna de melincue.

[44] United State Department of Agriculture. Soil bulk density, Moisture, Areation.